

Estimating Regional Deformation from a Combination of Space and Terrestrial Geodetic Data

D. Dong¹, T. A. Herring², and R. W. King²

¹ Jet Propulsion Laboratory, 4800 Oak Grove Dr., Pasadena, California 91109

² Department of Earth, Atmospheric, and Planetary Sciences, Massachusetts Institute of Technology, Cambridge, Massachusetts 02139

Abstract. We discuss an approach for efficiently combining different types of geodetic data to estimate time-dependent motions of stations in a region of active deformation. The primary observations are analyzed separately to produce loosely constrained estimates of station positions and coordinate system parameters which are then combined with appropriate constraints to estimate velocities and co-seismic displacements. We define a non-integer number of degrees of freedom to handle the case of finite constraints and stochastic perturbation of parameters and develop statistical tests for determining compatibility between different data sets. With these developments, we show an example of combining space and terrestrial geodetic data to obtain the deformation field in southern California.

Keywords: Deformation analysis, Estimation, Space geodesy

Address for correspondence: Dr. Danan Dong
JPL 238-332
4800 Oak Grove Dr
Pasadena, CA 91109
Phone 1-818-393-1827
Fax 1-818-393-6890
E-mail dong@freia.jpl.nasa.gov

1. Introduction

Studying the kinematics of the Earth's crust is a complicated problem for which geodetic measurements provide important constraints. Though dominated today by GPS data, these studies can take advantage of terrestrial measurements, particularly high precision electronic distance measurements (EDM) concentrated across active faults, and global satellite laser ranging (SLR) and very long baseline interferometry (VLBI) observations spanning over a decade. The availability of global GPS observations and the need to use the orbital information from these in the analysis of regional networks further motivates efforts to develop efficient methods of combining data. In this paper, we discuss an approach to estimating a crustal deformation field that addresses both the efficient use of global GPS data in the analysis of regional networks and the combination of GPS and terrestrial survey data.

We perform our analysis in three steps. First, we obtain loosely constrained estimates of geodetic parameters from space-geodetic or terrestrial observations from individual experiments. Second, we combine the individual loosely constrained estimates into a single solution, estimating station velocities and allowing stochastic variation of station coordinates and orbital and Earth rotation parameters when appropriate. Third, we impose general constraints in position and velocity to define a uniform reference frame. This methodology allows us to 1) perform simultaneous reduction with various types of geodetic data, 2) combine rigorously global and regional observations, 3) process efficiently and flexibly large volumes of data, and 4) estimate time-dependent displacements from earthquakes or changes in instrumentation. Several important byproducts, such as the strain rates and rotation rates over the whole network or subnetworks, are also obtained from the final velocity solutions [Feigl *et al.*, 1993].

Aggregation of data using saved normal equations or estimates with variance-covariance matrices has a long history in the analysis of both terrestrial and space-based geodetic data. More recently, it has become a key element in the program of coordinated GPS analysis conducted under the auspices of the International GPS Service for Geodynamics (IGS) [Beutler *et al.*, 1994; Blewitt *et al.*, 1993]. In this paper we focus on problems that arise when terrestrial and space-based data are combined, and on the computation of appropriate statistics in the presence of finite constraints and state perturbations. We also document in detail the algorithms incorporated in the GLOBK [Herring, 1995] and FONDA [Dong, 1993] softwares which have been widely used for studies involving global geodynamics [Herring *et al.*, 1991], regional strain rate [Feigl *et al.*, 1993; Oral *et al.*, 1995; Bawden *et al.*, 1996], and

co-seismic deformation [Bock *et al.*, 1993; Hudnut *et al.* 1994; Bennett *et al.*, 1995; Hudnut *et al.* 1996]. Finally, we present an example of combining trilateration and GPS measurements in southern California.

2. Analyzing the primary observations

A rigorous combination of various geodetic data does not necessarily require that the original, or primary observations be analyzed simultaneously. It is necessary only that the variance-covariance matrices carried forward from the separate analyses include all the parameters that are common to more than one subset of the data. In combining GPS, SLR, and VLBI observations, for example, parameters of the Earth's rotation should be included; in combining space-geodetic and terrestrial data, it is usually necessary to retain only station coordinates and velocities. In our three-step approach, the estimated parameters from the analysis of the primary observations become quasi-observations for the second step. The combination of different observation types or data from multiple epochs is implemented through the quasi-observations.

Our mathematical framework is four-dimensional integrated geodesy, which embodies the intrinsic correlation between the Earth's shape and its gravitational potential. The formalization can be found in the work of *Hein* [1986] and *Collier et al.* [1988]. To avoid unnecessary complexity, we simplify the formulas by omitting parameters which are not used for studying horizontal crustal deformation. On the other hand, we express the time dependence of station position vector with a linear model, considering episodic station displacements and allowing a stochastic representation of post-seismic relaxation.

By omitting the time-dependent disturbing potential, the geodetic measurement $l(t)$ can be expressed as

$$l(t) = F\{\mathbf{X}(\mathbf{a},t),U(\mathbf{X}(\mathbf{a},t)),\mathbf{h}(t)\} \quad (1)$$

where

$\mathbf{X}(\mathbf{a},t)$ is the position vector, whose time-dependency is described by the parameters \mathbf{a} ;

$U(\mathbf{X}(\mathbf{a},t))$ is the reference gravitational potential, with the time-dependent disturbing potential excluded;

$\mathbf{h}(t)$ are auxiliary parameters, representing propagation effects, satellite positions, etc.; and

F denotes a non-linear functional which operates upon \mathbf{X} , U , and \mathbf{h} to produce the scalar value of $l(t)$.

For a wide variety of observations (e.g., trilateration, chord distances, and space-based measurements) there is little or no dependence on local U; for others (e.g., triangulation and leveling), there is a strong dependence.

The linearized observation equation is

$$\delta l = A \Delta \mathbf{X}(\mathbf{a}, t) + B \Delta U(\mathbf{X}_0) + C \Delta \mathbf{h}_0 + \varepsilon \quad (2)$$

where

δl represents the residual of observed minus calculated, based on the a priori model;

$\Delta \mathbf{X}(\mathbf{a}, t)$ is the adjustment of time-dependent position vector;

$\Delta U(\mathbf{X}_0)$ is the correction to the reference potential at a priori position \mathbf{X}_0 ;

$\Delta \mathbf{h}_0$ is the correction of the a priori auxiliary parameter \mathbf{h}_0 ; and

ε represents the errors in the observations.

$$A = \frac{\partial F}{\partial \mathbf{X}} + \frac{\partial F}{\partial U} \frac{\partial U}{\partial \mathbf{X}} \quad B = \frac{\partial F}{\partial U} \quad C = \frac{\partial F}{\partial \mathbf{h}} \quad (3)$$

In the analysis of the primary observations, the variations of estimated $\Delta \mathbf{X}(\mathbf{a}, t)$ carry the crustal deformation information, which will be explicitly parameterized and estimated in the next step. In general, the potential parameters can be estimated simultaneously with other parameters [Milbert and Dewhurst, 1992]. In determining horizontal motion, however, it is sufficient to use the potential terms in (2) to perform corrections to those observations which are sensitive to the gravitational field. Appendix A lists the linearized observation equations for various geodetic measurements.

The reference frame in which the primary observations are analyzed depends on the nature of the measurement technique. Space-based measurements usually require an inertial ("celestial") frame, with origin at the geocenter for observations of near-Earth satellites (SLR, GPS) or the solar-system barycenter for observations of the Moon or extragalactic radio sources (VLBI). The coordinates of the stations are transformed by applying matrix rotations accounting for precession, nutation, polar motion, and the Earth's diurnal rotation, and by applying, if necessary, vector translations of the origin (see *IERS* [1992]). Terrestrial surveys measure distance, angle, orientation and height between stations, using the geoid to define the local horizontal and vertical directions. Geodetic or local topocentric coordinates used in these measurements may be transformed to geocentric coordinates using standard equations (see, e.g., Vanicek and Krakiwski [1986]). For simplicity, and greatest convenience in the analysis of space-geodetic observations, we express all coordinates using Cartesian components in a geocentric, Earth-fixed frame.

In analyzing the primary observations, we apply loose constraints to all of the parameters to be carried forward as quasi-observations. By not tightly constraining any of the parameters, we allow the reference frame to be defined consistently after combination [Herring *et al.*, 1991; Hefflin *et al.*, 1992]. On the other hand, some constraint is necessary to prevent the normal matrix from becoming singular. The constraint should be weak enough so as not to affect the parameter estimates, but not so weak as to cause significant rounding error in the computations. If the parameter estimates are uncorrelated, the change in the adjustment due to the constraint being applied is proportional to the ratio of the a posteriori variance, in the absence of a constraint, to the a priori variance of the parameter estimates [see Herring *et al.*, 1990]. That is, if the a priori variance is 1000 times greater than the a posteriori variance of the parameter, the effect on the estimates should be about one thousandth of the size of the adjustment. In practice, correlations between parameters lead to greater sensitivity to the a priori constraints. In the limit of high correlations among all the parameters, the effect of the constraint is n times larger than the uncorrelated case, where n is the number of parameters in the analysis. Analyses of GPS data shows that for solutions in which some of the stations are tightly constrained, the effects of constraints on the other stations are very similar to predictions from the uncorrelated case given in Herring *et al.* We show results for a loosely constrained analysis in Figure 1. In this case, the simple uncorrelated rule underestimates the effects by up to a factor of two but this factor is still far less than the several hundred potentially highly correlated parameters in this analysis.

A practical advantage of our approach is the saving in computation time and data storage. The loosely constrained solutions contain all the geodetic information in the primary data, but in a much compressed form. For example, data from a single GPS observation session may consist of phase measurements from 20 stations accumulated at 30-second intervals over 24 hours. For this case the files required to store the residuals and the partial derivatives with respect to station coordinates and satellite parameters typically occupy about 20 Mb of storage. In the quasi-observation approach, we need to keep only the estimated station coordinates, satellite orbits, earth rotation parameters, and their covariance matrix, which are easily stored in about 2 Mb. Computation time for the combination is typically reduced by about two orders of magnitude. Quasi-observations are not sufficient, however, if a need arises to change the model used to analyze the primary observations.

3. Combining data using Quasi-observations

In the second step of our analysis, we treat the estimated $\Delta\mathbf{X}(\mathbf{a},t)$ from individual subsets of data as quasi-observations to estimate station positions as a function of time;

$$\Delta\mathbf{X}(\mathbf{a},t) = (1+\lambda)\Delta\mathbf{X}_0 + (t-t_0)\Delta\mathbf{V}_0 + \sum_k r_k(t,t_k)\delta\xi_k + \boldsymbol{\gamma}(t) + \boldsymbol{\tau}_x + (t-t_0)\boldsymbol{\tau}_v + \boldsymbol{\mu}\boldsymbol{\omega}_x + \boldsymbol{\mu}(t-t_0)\boldsymbol{\omega}_v \quad (4)$$

where the parameter vector \mathbf{a} is embodied by \mathbf{V} , $\boldsymbol{\xi}$, $\boldsymbol{\gamma}$, $\boldsymbol{\tau}_x$, $\boldsymbol{\tau}_v$, $\boldsymbol{\omega}_x$, $\boldsymbol{\omega}_v$, λ defined below,

$\Delta\mathbf{X}_0$, $\Delta\mathbf{V}_0$ are the adjustments to the a priori coordinates and velocities referred to an reference epoch t_0 ;

$\delta\xi_k$ is the episodic station displacement from the k -th event, at time t_k , with

$$r_k(t,t_k) = \begin{cases} -1 & \text{if } t < t_k < t_0 \\ 0 & \text{if } t > t_k, t_k < t_0 \text{ or } t < t_k, t_k > t_0 \\ 1 & \text{if } t > t_k > t_0 \end{cases} \quad (5)$$

$\boldsymbol{\gamma}(t)$ is a stochastic displacement due, for example, to post-seismic motion or a short-term monument instability.

λ is the scale correction factor,

$\boldsymbol{\tau}_x$ and $\boldsymbol{\tau}_v$ are the translation and its rate of the network;

$\boldsymbol{\omega}_x$, $\boldsymbol{\omega}_v$ represents a rotation and rotation rate of the network or, equivalently for global observations, the Earth rotation and rotation rate parameters, with

$$\boldsymbol{\mu} = \begin{pmatrix} 0 & -z_0 & y_0 \\ z_0 & 0 & -x_0 \\ -y_0 & x_0 & 0 \end{pmatrix} \quad (6)$$

in which x_0 , y_0 , z_0 are the a priori coordinates;

Thus the three elements of a dynamic reference system position relative to a specified epoch, velocity, and episodic displacement are estimated simultaneously.

Both classical least squares and stochastic estimators provide a natural framework for combining data from multiple epochs and different types of observations. In least squares these are represented by the normal equations; in sequential estimators by parameter estimates and their covariance matrices. In order to treat the most general case, we present our approach in terms of the equations for a Kalman filter, of which sequential least squares is a special case. Alternative formulations in terms of batch least squares, a U-D factorization covariance filter, or square-root information filter (SRIF) commonly used in spacecraft navigation can also be derived [*Bierman, 1977; Blewitt et al, 1993*].

Let $\delta\mathbf{l}_k = \mathbf{l}_k - \mathbf{l}_{0k}$ be the vector of linearized quasi-observations at time t_k , where \mathbf{l}_{0k} represents the a priori values and \mathbf{l}_k the estimates of the quasi-observations from the analysis of the original observations. The observation equation is

$$\delta\mathbf{l}_k = \mathbf{A}_k \delta\mathbf{x}_k + \boldsymbol{\varepsilon}_k \quad (7)$$

in which \mathbf{x}_k are the parameters to be estimated (e.g., from the right-hand side of Eq. (4)), \mathbf{A}_k is the design matrix of partial derivatives, and $\boldsymbol{\varepsilon}_k$ is a zero-mean, white-noise process with covariance \mathbf{P}_k . The parameter state is represented by

$$\delta\mathbf{x}_{k+1} = \mathbf{S}_k \delta\mathbf{x}_k + \mathbf{q}_k \quad (8)$$

where \mathbf{S}_k is the state-transition matrix representing the dynamic evolution of the parameters and \mathbf{q}_k is a Markov stochastic process with covariance \mathbf{Q}_k . In our case \mathbf{S}_k is usually just the relationship between position at t_{k+1} and position and velocity at t_k . To estimate the parameters at time t_{k+1} , one first propagates the estimates and their covariance,

$$\delta\widehat{\mathbf{x}}_{k+1|k} = \mathbf{S}_k \delta\widehat{\mathbf{x}}_k \quad (10a)$$

$$\mathbf{C}_{k+1|k} = \mathbf{S}_k \mathbf{C}_k \mathbf{S}_k^T + \mathbf{Q}_k \quad (10b)$$

and then updates the estimates using the current observations,

$$\delta\widehat{\mathbf{x}}_{k+1} = \delta\widehat{\mathbf{x}}_{k+1|k} + \mathbf{K}_{k+1} (\delta\mathbf{l}_{k+1} - \mathbf{A}_{k+1} \delta\widehat{\mathbf{x}}_{k+1|k}) \quad (11a)$$

$$\mathbf{C}_{k+1} = \mathbf{C}_{k+1|k} - \mathbf{K}_{k+1} \mathbf{A}_{k+1} \mathbf{C}_{k+1|k} \quad (11b)$$

where

$$\mathbf{K}_{k+1} = \mathbf{C}_{k+1|k} \mathbf{A}_{k+1}^T (\mathbf{P}_{k+1} + \mathbf{A}_{k+1} \mathbf{C}_{k+1|k} \mathbf{A}_{k+1}^T)^{-1} \quad (12)$$

is the "Kalman gain" matrix. In these equations, $k+1|k$ denotes the prediction at t_{k+1} using data through t_k , and the superscript T denotes the transpose of a vector or matrix. Since the new covariance matrix is obtained by decrementing the old one, numerical instabilities can arise if the a priori uncertainties are too large or the propagated covariance becomes too large due to the use of large values of the Markov parameters. This latter situation sometimes occurs, for example, when station coordinates are considered as stochastic parameters (e.g., to test repeatability) and two observations are separated by long periods of time. The rule of thumb discussed in the previous section can be used to determine the appropriate level of constraint.

The scalar "weighted sum of squared residuals" (χ^2) is widely used in least squares analysis as an indicator to rescale the a posteriori uncertainty, detect observation blunders, test the compatibility of different data sets, and to assess the significance of different parameterizations [Segall and Matthews, 1988]. To apply this scalar in the general case of Kalman filtering, we define the increment of $\delta\chi^2$ as

$$\delta\chi_{k+1}^2 = \chi_{k+1}^2 - \chi_k^2 = (\delta\mathbf{l}_{k+1} - \mathbf{A}_{k+1} \delta\widehat{\mathbf{x}}_{k+1})^T \mathbf{P}_{k+1}^{-1} (\delta\mathbf{l}_{k+1} - \mathbf{A}_{k+1} \delta\widehat{\mathbf{x}}_{k+1}) + \Delta\widehat{\mathbf{x}}_{k+1}^T \mathbf{C}_{k+1|k}^{-1} \Delta\widehat{\mathbf{x}}_{k+1} \quad (13)$$

$$\text{where } \Delta\widehat{\mathbf{x}}_{k+1} = \delta\widehat{\mathbf{x}}_{k+1} - \delta\widehat{\mathbf{x}}_{k+1|k} = \delta\widehat{\mathbf{x}}_{k+1} - \mathbf{S}_k \delta\widehat{\mathbf{x}}_k \quad (14)$$

The first term of (13) represents the increment in χ^2 from adding new data, and the second term represents the increment as the solution is propagated forward to a new epoch. In Appendix B, we show that in the case of time-invariant parameters ($\delta\widehat{\mathbf{x}}_{k+1|k} = \delta\widehat{\mathbf{x}}_k$, $\mathbf{C}_{k+1|k} = \mathbf{C}_k$), (13) is equivalent to the classical definition of $\delta\chi^2$. The definition (13) can also be expressed in the form (see Appendix B)

$$\delta\chi_{k+1}^2 = (\delta\mathbf{l}_{k+1} - \mathbf{A}_{k+1}\delta\hat{\mathbf{x}}_{k+1|k})^T (\mathbf{P}_{k+1} + \mathbf{A}_{k+1}\mathbf{C}_{k+1|k}\mathbf{A}_{k+1}^T)^{-1} (\delta\mathbf{l}_{k+1} - \mathbf{A}_{k+1}\delta\hat{\mathbf{x}}_{k+1|k}) \quad (15)$$

Since (15) uses only the propagated estimates $\delta\hat{\mathbf{x}}_{k+1|k}$, it allows estimation of the increment of χ^2 before Kalman filtering, which is quite useful for identifying and eliminating outliers in combining a large number of quasi-observations and also in navigation and real-time deformation analysis, where the solution is derived from processing the primary observations. Our software uses (15) to compute the increments in χ^2 during filtering (although the degrees of freedom are not computed completely during the filtering stage). Note that (15) can lose its sensitivity if the initial propagated covariance, $\mathbf{C}_{k+1|k}$, is too large.

4. Imposing general constraints

The constraints impose additional information on the estimated parameters. Their function is threefold: i) to remove the rank deficiency, which exists inherently in both terrestrial and space-geodetic data; ii) to define a uniform reference frame through the well-determined stations common to all experiments; and iii) to take advantage of a priori knowledge to strengthen the combination solution. In deformation analysis, the most commonly used constraints equate the adjustments of parameters. Inequality constraints can also be used by transforming them into the unconstrained problem via a penalty function [Zhao and Sjöberg, 1995].

After combining the loosely constrained quasi-observations, the reference frame of the combination solution is only weakly established. This frame has (effectively) a twelfth-order rank deficiency: three translations, three rotations, and their rates. How we remedy the rank deficiency and define the reference frame depends on what kind of data we have and how much a priori knowledge we can utilize. All geodetic observations have a rotational uncertainty and some, such as VLBI and EDM, have a translational deficiency. For GPS there is theoretically no translational rank deficiency since the orbital dynamics are sensitive to the position and velocity of the Earth's center of mass, but a weak global tracking network and/or poor modeling of the orbital dynamics often encourage us to constrain the translation and its rate to stabilize the solution. None of the observations is degenerate in scale, but all have errors that may encourage us to constrain the scale. For VLBI, scale errors can arise from deficiencies in modeling atmospheric delays [MacMillan and Ma, 1996]; while for GPS, from antenna phase center models, atmospheric delay models and deficiencies in modeling satellite orbital dynamics; and for EDM, from calibration of meteorological probes and the frequency standards used in the measurement equipment. In Appendix E we discuss our approach to

defining rotation, translation, and scale for geodetic networks. We also show that for systems such as GPS, which are strictly not free to translate or re-scale, it may still be necessary to estimate translation and scale parameters explicitly in order to minimize the effects of modeling errors on the estimated station coordinates.

Trilateration and triangulation data cannot resolve the translation and rotation and their rates of the entire network. Triangulation data are also insensitive to the scale of the network. Traditionally, there are two approaches to deal with the rank deficiency when only terrestrial data are available. One approach is to estimate regional strain rates instead of velocities under the assumption that the strain variation is uniform in time and the velocity gradient is constant over the network. Such a parameterization gives uniquely determined parameter estimates [Bibby, 1982; Drew and Snay, 1987]. For noisy data, this parameterization provides spatially averaged results to enhance the signal-to-noise ratio. This approach is most suitable for a small area, where the assumption of a spatially uniform velocity gradient is valid. A large or tectonically complicated area must be divided into smaller districts, based on a priori knowledge, to implement this approach. The velocity field is obtained by integrating the velocity gradient from a station with a known or assumed velocity. The derived velocities are highly correlated. An alternative approach is to use external constraints to eliminate the rank deficiency. This approach removes the assumption of a spatially uniform velocity gradient. The "inner coordinate solution" [Brunner, 1979] represents the minimum-norm generalized inverse of a singular normal matrix, and assumes the prior model to be zero. The "outer coordinate solution" [Prescott, 1981] constrains network rotation such that the velocities along a specified direction are minimized. The "model coordinate solution" [Segall and Mathews, 1988] applies the velocity field derived from a geophysical model to constrain the solution. Both "outer coordinate" and "model coordinate" solutions usually match well the known local tectonic features. They are especially useful when we want to calibrate or quantify the model parameters. Nevertheless, in a tectonically complicated region it is difficult to specify a single dominant direction to apply outer coordinate constraints or to construct a model velocity field in advance. As a result, these methods are also applied best to small areas. Combining terrestrial survey data with space geodetic data makes it possible to derive an unambiguous estimate of station velocities over a large area [Snay and Drew, 1989; Grant 1990; Dong 1993]. If derived using data from a global network, the space-geodetic solution can be considered unambiguous on a regional scale, allowing the space-geodetic and terrestrial estimates of horizontal velocities at collocated stations to be linked to remove the rank deficiency in terrestrial measurements. If the offsets between the instrumental reference

points used by different techniques are known, we can link the coordinate estimates at these collocated stations, thus providing additional information (see, e.g., *Feigl et al.* [1993]).

We apply constraints in our analysis by treating them as quasi-observations [e.g. *Jackson*, 1979], which are formally expressed as

$$\mathbf{l}_c = \mathbf{A}_c \delta \mathbf{x} + \boldsymbol{\varepsilon}_c \quad \text{with covariance } \mathbf{C}_c \quad (16)$$

Suppose that the parameter adjustments from the combined, loosely constrained solutions are $\widehat{\delta \mathbf{x}}$ with covariance \mathbf{C}_x and misfit χ_x^2 , then the solution, covariance and misfit after the constraints become

$$\widehat{\delta \mathbf{x}}_c = \widehat{\delta \mathbf{x}} + \mathbf{C}_x \mathbf{A}_c^T (\mathbf{C}_c + \mathbf{A}_c \mathbf{C}_x \mathbf{A}_c^T)^{-1} (\mathbf{l}_c - \mathbf{A}_c \widehat{\delta \mathbf{x}}) \quad (17)$$

$$\mathbf{C}_{x_c} = \mathbf{C}_x - \mathbf{C}_x \mathbf{A}_c^T (\mathbf{C}_c + \mathbf{A}_c \mathbf{C}_x \mathbf{A}_c^T)^{-1} \mathbf{A}_c \mathbf{C}_x \quad (18)$$

$$\chi_c^2 = \chi_x^2 + (\mathbf{l}_c - \mathbf{A}_c \widehat{\delta \mathbf{x}})^T (\mathbf{C}_c + \mathbf{A}_c \mathbf{C}_x \mathbf{A}_c^T)^{-1} (\mathbf{l}_c - \mathbf{A}_c \widehat{\delta \mathbf{x}}) \quad (19)$$

Setting $\mathbf{C}_c = 0$ in (16) is the classical "hard" constraint (also called an "absolute" constraint by *Vanicek and Krakiwsky* [1986]), which is equivalent to fixing some linear combinations of the parameters to specified values or making some parameters have exactly the same adjustment. When $\mathbf{C}_c > 0$ in (16), this case represents a "soft" or "weighted" constraint [*Vanicek and Krakiwsky*, 1986], which allows the parameter adjustments to differ by an amount controlled by \mathbf{C}_c . Thus, \mathbf{C}_c functionally characterizes the perfectness ("hardness") of a priori knowledge about the constraint. The soft constraint is useful when our knowledge about the constraints is not perfect; that is, if the constraints are based on other observational estimates rather than on rigorous theoretical formula. It also has considerable utility in deformation analysis, for example in accounting for differences between two measurements due to viscoelastic relaxation or afterslip following an earthquake.

With the three-step approach, we can manipulate various constraints without reprocessing the original observation data. The reasonableness of the constraints can be assessed from the increments of χ^2 (Eq. (19)). A variety of constraints useful in the deformation analysis can be found in *Dong* [1993]; some of these will be discussed in our example.

5. Statistical tests of the combined solution

In the combination, the covariance matrices of the different data sets should reflect both the internal uncertainties and the uncertainties of biases between them. Determining the appropriate relative weight between different data sets requires external knowledge or

extensive comparisons, which are beyond the scope of this paper. We can, however, discuss the tools used to assess the statistical compatibility of the individual quasi-observations.

Davis et al. [1985] have shown that for the same parameters with the addition of new data uncorrelated with previous data, the covariance matrix of differences of the parameter estimates has the relation

$$\mathbf{C}_{\tilde{\mathbf{x}}-\hat{\mathbf{x}}} = \mathbf{C}_{\hat{\mathbf{x}}} - \mathbf{C}_{\tilde{\mathbf{x}}} \quad (20)$$

where $\tilde{\mathbf{x}}$ and $\hat{\mathbf{x}}$ denote the estimated parameters with and without new data added, respectively. Equation (20) is often used to check the compatibility of new data with the original data (estimating the same parameters) or to test the sensitivity of parameter estimates to subsets of data. The difference between (C.18) of Appendix C and (20) indicates that adding additional parameters enlarges the covariance of common parameters for the same data, whereas (20) shows that for the same parameters, adding new data reduces the estimated covariance.

Formula (20) can be extended to a general case not only when new data are added, but also when additional parameters are estimated, provided that the new data are uncorrelated with the previous data and the new parameters depend only on the new data (see proof in Appendix D). We further extend the formula to a more general case by allowing time-variant parameters and state perturbation. The corresponding formula is

$$\mathbf{C}_{\hat{\mathbf{x}}_{k+1}-\hat{\mathbf{x}}_{k+1|k}} = \mathbf{C}_{k+1|k} - \mathbf{C}_{k+1} \quad (21)$$

A straightforward extension of (21) is

$$\mathbf{C}_{L(\hat{\mathbf{x}}_{k+1}-\delta\hat{\mathbf{x}}_{k+1|k})} = \mathbf{C}_{L(\hat{\mathbf{x}}_{k+1|k})} - \mathbf{C}_{L(\hat{\mathbf{x}}_{k+1})} \quad (22)$$

where $L(\mathbf{x})$ in (22) represents any linear transformation of \mathbf{x} . In the example of this paper, (22) is used to set the criterion that if the solution difference $L(\hat{\mathbf{x}}_{k+1}-\delta\hat{\mathbf{x}}_{k+1|k})$ exceeds the 95% confidence level, an incompatibility between different data sets is detected. Formula (21) can be further extended to the smoothed Kalman filtering solution [see *Herring et al.*, 1990] from the forward and backward running Kalman filter (see Appendix D). Formulas (20) to (22) are applied to the covariance and adjustments as a whole and the compatibility test should be performed strictly in a multi-dimensional Hilbert space. In practice, however, it is less useful to have a rigorous measure of compatibility than to identify the stations causing the problem. Hence, we usually perform the tests on the coordinate and velocity adjustments for each station separately, neglecting the correlations between parameters of different stations and between coordinates and velocities [see Appendix of *Feigl et al.*, 1993].

Incompatibilities can arise from incomplete editing of the data, unmodeled systematic errors, reference frame constraints implemented differently in different data sets, underestimated noise covariances, and overly tight constraints. A shortcoming of (22) is that many incompatibilities are caused by the inconsistencies in the data, but this test is performed in parameter space. There is unfortunately no one-to-one correspondence between data space and parameter space. The error in one data component or in one constraint can smear the entire solution and thus make innocent parameters appear incompatible. Identifying the inconsistent data must be accomplished by returning to the analysis of the primary observations after narrowing the candidate surveys using the $\delta\chi^2$ as the quasi-observations are added to the combination. After removing blunders, an abnormally large $\delta\chi^2$ usually indicates unmodeled systematic error, or that we have underestimated the effective data noise, perhaps by ignoring temporal correlations. Rescaling the covariance matrix on the basis of the effective uncorrelated sampling rate provides a reasonable, if not rigorous, means of obtaining realistic uncertainties. [see, e.g. *Feigl et al.*, 1993; more rigorous approaches for continuous GPS data are discussed in *King et al.*, 1995 and *Zhang et al.*, 1996b]. External checking based on prior geophysical information is also helpful in detecting the potential errors in network rotation and translation [see p. 38 of *Dong*, 1993].

The misfit χ_x^2 (defined in (3.7)) obeys the χ^2 -distribution with $n-m$ degrees of freedom, where n is the observation number, and m is the estimated parameter number ($n > m$). If the true variance is known, the character of χ_x^2 is applied to perform statistical tests of the mathematical model. In most deformation analyses, researchers tend to accept a mathematical model that makes physical sense, and to consider the true variance as unknown. Then the a posteriori uncertainty is rescaled by the normalized root-mean-square (nrms):

$$\text{nrms} = \sqrt{\frac{\chi_x^2}{n - m}} \quad (23)$$

When imposing k general constraints (defined in (16)), the misfit χ_c^2 with constraints can be calculated by (19). In the case of "hard" constraint ($C_c \rightarrow 0$), the increment of χ^2 becomes

$$\Delta\chi^2 = \chi_c^2 - \chi_x^2 = (\mathbf{I}_c - \mathbf{A}_c \delta\hat{\mathbf{x}})^T (\mathbf{A}_c \mathbf{C}_x \mathbf{A}_c^T)^{-1} (\mathbf{I}_c - \mathbf{A}_c \delta\hat{\mathbf{x}}) \quad (24)$$

which also obeys the χ^2 -distribution with k degrees of freedom and is statistically independent of χ_x^2 [*Caspary*, 1987]. Such a character is conventionally applied to test the reasonableness of the constraint by either a χ^2 - test (when the true variance is known) or an F- test (when the true variance is unknown).

The introduction of soft constraints complicates the statistical character of χ_c^2 , as can be seen from the following two extremes. When the constraints are very "soft" ($C_c \rightarrow \infty$ in (16)), the solutions are virtually undisturbed (note (17), (18), (19) with $C_c = \infty$). Hence χ_c^2 still obeys the χ^2 - distribution with $n-m$ degrees of freedom. When the constraints are very "hard" ($C_c \rightarrow 0$), χ_c^2 also obeys χ^2 - distribution but with $n-m+k$ degrees of freedom. Here we implicitly assume the rank of A_c is k to eliminate the case of completely correlated absolute constraints. In order to perform this test formally for general weighted constraints ($0 \leq C_c \leq \infty$), we consider that χ_c^2 obeys approximately a χ^2 - distribution but with $n-m+e$ degrees of freedom ($0 \leq e \leq k$), where $(n-m+e)$ is in general no longer an integer. Here e represents the reduced estimated parameter dimension due to the constraints on parameters. It must satisfy the following three conditions:

- (i) When $C_c \rightarrow \infty$, $e \rightarrow 0$.
- (ii) When $C_c \rightarrow 0$, $e \rightarrow k$. Here k is the rank of A_c .
- (iii) In general, $0 \leq e \leq k$.

When the estimated parameters are uniquely determined, which is the case in deformation analysis (rank deficiency is always remedied by constraints), the resolution matrix [Jackson, 1979] is the identity matrix with dimension of m . It consists of two parts:

$$I = R_d + R_c = N^{-1}A^T C_l^{-1}A + N^{-1}A_c^T C_c^{-1}A_c \quad (25)$$

$$\text{where } N = A^T C_l^{-1}A + A_c^T C_c^{-1}A_c \quad (26)$$

and R_d , R_c represent the contributions to the resolution matrix from data and constraints respectively. We define e as the trace of the sub-resolution matrix R_c :

$$e = \text{trace}(R_c) = \sum_i (R_c)_{ii} \quad (27)$$

It can be found that e satisfies the conditions (i) (see (25)) and (ii) (see (18)). For a special case of $A_c = (0, I_k)$, Jackson and Matsu'ura [1985] proved that $0 \leq (R_c)_{ii} \leq 1$ for each of the k constrained parameters, which denotes the share of contribution to the parameter from the constraint. For a general A_c , the individual $(R_c)_{ii}$ could exceed the range between zero and one, but the sum of $(R_c)_{ii}$ is still between 0 and k [Shen, 1991]. Thus the defined e also satisfies the condition (iii). Note that no matter how many constraints have been imposed, e never exceeds the parameter dimension m since the $\text{rank}(A_c) \leq m$, that makes sense because all our constraints are imposed in the parameter space.

The state perturbation noise \mathbf{q}_k performs a role opposite that of the constraints. If its covariance $\mathbf{Q}_k \rightarrow \infty$, all the corresponding parameters are effectively reset at epoch k , implying the degrees of freedom are reduced by the number of reset parameters. If its

covariance $\mathbf{Q}_k \rightarrow 0$, no parameter is perturbed, implying no change in the degrees of freedom. If the real number p_k represents the degrees of freedom reduced by the state perturbation noise at epoch k , it must satisfy the following three conditions:

- (i) When $\mathbf{Q}_k \rightarrow \infty$, $p_k \rightarrow 0$.
- (ii) When $\mathbf{Q}_k \rightarrow 0$, $p_k \rightarrow j$, where j is the rank of \mathbf{Q}_k .
- (iii) In general, $0 \leq p_k \leq j$.

$\mathbf{C}_{k+1|k}^{-1} \mathbf{Q}_k$ satisfies the above conditions (see (10b)). However, $\mathbf{C}_{k+1|k}^{-1} \mathbf{Q}_k$ requires the inverse of the full covariance matrix at every time propagating step, which is time consuming and conflicts with our goal of efficiency. Note that in deformation analysis, \mathbf{Q}_k is usually a diagonal or block diagonal matrix. If $\mathbf{C}_{k+1|k}^*$ and \mathbf{Q}_k^* represent the matrices $\mathbf{C}_{k+1|k}$ and \mathbf{Q}_k with all off-diagonal terms set to zero, $\mathbf{C}_{k+1|k}^{*-1} \mathbf{Q}_k^*$ also satisfies the above conditions but with greater computational efficiency. In this paper, p_k is defined as the trace of $\mathbf{C}_{k+1|k}^{*-1} \mathbf{Q}_k^*$. Thus the number of degrees of freedom is defined by

$$n - m + e - \sum_k p_k \quad (28)$$

The degrees of freedom are further complicated by the quasi-observations. Unlike the analysis of primary data, the number of observations (n in (28)) does not necessarily equal to the number of quasi-observations. For example, we can estimate n station coordinates as n quasi-observations from a GPS campaign data spanning a few days. For the same GPS campaign data, we may also estimate n station coordinates and n station velocities to formally obtain $2n$ quasi-observations. However, the n station velocities are actually "virtual" quasi-observations with little resolution from the data, and hence should be excluded from the number of observations. The appropriate number of observations should be the data-contributed resolution part of the quasi-observations (R_d in (25)) and therefore is a real-value in general. In practice, the number of loosely constrained GPS campaign quasi-observations (station coordinates only) can be treated as the number of observation assuming that the very weak stations have been excluded. For the loosely constrained EDM quasi-observations, however, the data contributed resolution matrix should be used to compute the appropriate number of observations because the rank deficiency and weak resolution for some parameters of the trilateration data (network translation, rotation and their rates, single baseline observations for some stations, limited resolution for the vertical coordinates and their rates) makes the data-contributed resolution always significantly smaller than the number of quasi-observations.

Definition (28) is based on the approximation that the classical χ^2 - distribution can be extended to a continuous function of the degrees of freedom. A more rigorous treatment

should include a theoretical discussion of the statistical distribution of χ_c^2 , and deduce its corresponding degrees of freedom from the distribution function. To our knowledge, this has not yet been done. We note that the three conditions for increasing the degrees of freedom by constraints and the three conditions for reducing the degrees of freedom by perturbations are necessary but not sufficient. Thus, we have provided a practical approach to performing statistical tests in the case of general constraints and state perturbation but have not resolved the problem completely.

6. Sub-optimal combination solutions

The rigorous combination of quasi-observations we have described will produce a solution identical to that obtained if all the original data are used simultaneously. The large increase in space geodetic data in recent years, particularly from continuously operating GPS stations, has led to many cases for which it is desirable to sacrifice a small degree of rigor in exchange for greater efficiency.

One example of a sub-optimal approach is the combination of data from a global GPS network with those from one or more regional networks. When double differences are used as observations, the networks can be connected with no redundancy by including a single common station between them, but the analysis will usually be sub-optimal because of the difficulty of dynamically choosing a common station that maximizes the number of independent baselines. In practice, it is usually desirable to introduce two or three common stations, accepting the factor of two increased weight given to baselines between these stations in exchange for the greater reliability achieved by not depending on flawless performance of a single common station. When one-way observations are used, sub-networking can be accomplished rigorously by including satellite clock parameters in each analysis, or sub-optimally by determining these parameters using a subset of the data.

In combining global and regional data, orbital parameters should be included in each analysis if the regional data can contribute significantly to the determination of orbits. Prior to 1994, global tracking stations were relatively sparse, allowing regional networks of a few hundred kilometers to make significant improvement in the estimates of the satellite's motion over the region [e.g., *Oral*, 1994]. With the current network of more than 50 globally distributed stations contributing to orbit determination by the IGS, regional networks of small aperture add little additional information to satellite parameters. Hence the regional stations

may be analyzed separately from the global tracking stations, with orbits fixed and correlations between the two solutions safely ignored [Zhang *et al.*, 1996a]. An extreme case using double differences is to analyze the observations one baseline at a time, making coordinate estimation in the phase analysis extremely fast but increasing the computation time of the combination. With one-way observations, estimation of station coordinates and clocks one station at a time may be accomplished by determining the satellite orbits and clocks from a global analysis [Zumberge *et al.*, 1996]. In either of these extreme cases, ignoring the correlations among the estimated coordinates may overestimate the uncertainties in the relative positions of the regional stations.

7. Combination of terrestrial and space-geodetic data in southern California

For southern California a rich and diverse set of terrestrial and space-geodetic data are available to measure crustal deformation. Triangulation began as early as the 1850s, trilateration with EDM in the 1950s, VLBI in the 1970s, and GPS in the 1980s (see e.g., Snay *et al.*, 1987; Hager *et al.*, 1991; Shen *et al.*, 1996). To illustrate the methodology developed in this paper, we have chosen a subset of the high-precision EDM data from 1972 to 1992 and GPS data acquired between 1986 and 1995 over a broad region from the western Transverse Ranges south to the Mexicali Valley (Figure 2). For this demonstration we have not reanalyzed the primary observations but rather used the previously analyzed quasi-observations of loosely constrained, time-dependent positions (Table 1).

During this period there were seven earthquakes large enough to affect the EDM or GPS measurements. In order to obtain robust estimates of both the velocities and co-seismic displacements for stations in the region, we imposed separately on the north, east, and vertical displacements a priori constraints of the form

$$\sigma(x) = \sqrt{[\sigma_e \times (\frac{d}{x})]^2 + \sigma_c^2} \quad (29)$$

where σ_e denotes the allowed displacement of the component at the earthquake epicenter, d the depth of the earthquake epicenter, x the distance between the epicenter and the surveyed station, and σ_c is independent of the distance from the hypocenter. Such a definition roughly approximates the expected coseismic displacements if the rupture is a screw dislocation in an elastic half space and the station is not very close to the epicenter. Stronger constraints can be applied by generating theoretical models for the earthquake from the seismic data or a set of near-field geodetic measurements. The importance of the coseismic constraint is the strength

it adds to the estimation of interseismic velocities, particularly those for stations several fault-depths away which have only a limited span of observations before and after the earthquake. The coseismic displacements can be estimated either explicitly (using $\sigma(x)$ as the a priori constraints for coseismic displacement parameters) or implicitly (using $\sigma(x)$ as the perturbations to the coordinate parameters when the quasi-observation epoch passing the earthquake occurrence epoch). The earthquake displacement features can also be used to account for monument instabilities [Dong, 1993]. In this case, only σ_c is used and applied to only specific components (e.g., height). The parameters used for each of the earthquakes in our region are given in Table 2.

For the Landers earthquake there is evidence from GPS observations of postseismic relaxation up to 55 mm for stations within 100 km from the fault within the first 34 days following the earthquake [Shen *et al.*, 1994]. In general, postseismic deformation is a complicated phenomenon with different spatial wavelengths and temporal relaxation spans and a simple exponential decay assumption may not be valid. Our software allows us to estimate different velocities for the periods before and after an earthquake, and to account for post-seismic relaxation by constraining the displacement parameters ($\gamma(t)$ in Eq. (4)) to obey a Markov process.

(a) EDM analysis

The EDM data used in this example were from the Joshua, Anza, Salton and part of the Monitor networks surveyed by the USGS from 1971 to 1992 [Lisowski *et al.* 1991]. The error model for the observations has the form $\sigma = \sqrt{a^2 + b^2 L^2}$ where L is the line length [Savage and Prescott, 1973]. This measurement uncertainty includes both a constant or instrumental component and a length-dependent component due to errors in the model used for atmospheric refraction and instrument frequency modulation. We used values of the coefficients ($a = 3$ mm and $b = 0.2$ ppm) determined by Savage *et al.* [1986] and reconfirmed by three recent analyses [Dong, 1993; Johnson *et al.*, 1994; Savage and Lisowski, 1995]. For the southern California networks used in our analysis, the intersite distances are 4 to 46 km, leading to uncertainties of 3 to 10 mm in measured line length. The EDM data used in this paper were precleaned with detected range busts had been corrected and the a priori coordinates of most EDM stations were updated based on more accurate collocated GPS station coordinates (see Appendices 10 and 13 of Dong [1993] for details). The coordinates at a small number of stations could not be updated since these stations had no sufficient baseline measurements. We set a criterion of 40 m to avoid coordinate

adjustments which could exceed the linear range. Three trilateration measurements were removed from a total of 2193 measurements.

The a priori constraints on horizontal coordinates and velocities at all stations were 20 m and 200 mm/yr respectively. Since the trilateration measurements have very limited sensitivity to vertical coordinate variations and the vertical length of EDM baselines is typically less than 10% of the horizontal length, we set 2 m and 20 mm/yr a priori constraints on vertical coordinates and velocities at all stations. Coseismic displacements from the first 6 earthquakes of Table 2 were estimated explicitly. There are several EDM stations which occupied the same benchmarks. Hence, the coordinate and velocity estimates at these stations were constrained to be equal. There are also several EDM stations located closely, usually within 100 meters. The velocity estimates at these stations were constrained to be the same. Thus, a total of 2189 EDM measurements were used to estimate 861 parameters (station coordinates, velocities and coseismic displacements) at 119 stations. Our assigned constraints reduced the effective number of estimated parameters by 344.96. The effective number of degree of freedom is 1672.96 and the postfit nrms is 1.22. This postfit nrms is consistent with the results of *Dong* [1993] and *Johnson et al.* [1994], in which they demonstrated that scatters of the linear fit of the EDM baseline measurements at the Anza, Joshua and Salton networks were about 10% to 20% larger than the nominal error model. Note that the EDM derived velocity field from the loosely constrained solution is poorly determined since we did not impose constraints on the network translation, rotation and their rates. However, the strain rates of this solution are well-determined. We extracted the velocity solution and its covariance matrix for 87 unique stations as the quasi-observation for the next stage GPS/EDM combination. The resolution matrix contributed from the constraints (complement to the contribution from the data) is also saved to compute the appropriate number of observations in the EDM/GPS combination.

(b) GPS analysis

The analysis of the GPS primary data used for this study is described in detail in *Feigl et al.* [1993], *Bennett* [1995], and *Hudnut et al.* [1996]. The error model is much less understood than for EDM, however, because the instrumentation, satellite constellation, global tracking network, and observing strategy have changed dramatically over the past decade. For the quasi-observations included in our analysis, there are four sources of systematic error known to be significant: inadequately modeled non-gravitational perturbations in the motions of the satellites; inadequately modeled atmospheric corrections, including a problem in the early software version leading to an incorrect elevation-angle dependence; oscillations

in phase due to reflection of the signal from the ground or nearby objects (multipathing); and unmodeled offsets and variations in the effective phase-centers of the receiving antennas. The orbital and atmospheric errors are roughly proportional to baseline length and tend to affect primarily the north and vertical coordinates. Multipathing and unmodeled antenna phase-center variations affect predominantly the vertical coordinates and are highly dependent on the local environment, type and separation of antennas, and the low-elevation cutoff of the observations or analysis. The magnitude of these errors can reach several centimeters in vertical coordinates but is usually only a few millimeters in horizontal coordinates. The processing of primary observations using the GAMIT software [King and Bock, 1995] assumed an a priori uncertainty of 10 mm in 30-s samples of (undifferenced) L1 and L2 carrier phase measurements (equivalent to 64 mm in the doubly differenced ionosphere-free combination). With this assumption, the nrms of the short-term scatter (over several days) of relative-position estimates is between 0.5 and 1.5 for most of the surveys included in our study, and the nrms of the long-term scatter (over several-years) is about 2 (see Feigl *et al.*, [1993], and Bennett [1995]). Feigl *et al.*'s comparison of GPS and VLBI estimates of station velocities also suggests that rescaling the GAMIT uncertainties by a factor of two is appropriate to obtain realistic one-sigma uncertainties from these data.

Most of the GPS analyses were carried out by combining phase observations from regional stations and as many North American or global stations as were available and estimating simultaneously station coordinates and orbital and Earth-orientation parameters. For the early surveys (1986 to 1991) in which only a limited number (3 to 10) of tracking stations was available, multiday orbital arcs were used to strengthen the orbit determination [Feigl *et al.*, 1993]. The 1988 Salton Trough survey (STRC88) had such poor global tracking that Bennett [1995] opted to use the broadcast ephemeris, constrained at the level of 5 parts in 10^7 . At the other extreme, Bennett analyzed the 1995 experiment without global tracking with the orbit he obtained from the Scripps Orbital Processing and Analysis Center (SOPAC) [SOPAC staff, 1996] being constrained at the level of 5 parts in 10^8 (1 m in orbital position). The 1993 Salton Trough survey was analyzed by using GLOBK to combine for each day quasi-observations (including orbital parameters) from the regional analysis with quasi-observations from a global analysis performed at SOPAC [Bennett, 1995]. The Intercounty 93 survey was divided into 4 subsets: global network, PGGGA network, regional with Ashtech receivers, and regional with Trimble receivers. Different network rotations and translations were allowed between the quasi-observations of the 4 subsets to reduce possible system inconsistencies from insufficient antenna phase center modeling and orbital modeling.

The 1990 Transverse Ranges survey (Trex18) also consisted of multiple antenna types (TI4100, MiniMac, and Trimble) but with no rotations or translations allowed between them.

Except for orbital constraints in the STRC88 and STRC95 analyses, all of the daily analyses were performed with loose constraints on all parameters, 20 to 50 meters for station coordinates, 10 parts per million for orbits, and 50 milliarcsecond (mas) for Earth-rotation parameters. These values are sufficiently large so that even with averaging over 500 stations, they bias the final coordinate adjustments (cm-level) by less than 0.01 mm. After forming quasi-observations from each daily analysis, we used GLOBK to combine these into a single set of quasi-observations for each survey. In this step, orbital parameters are no longer needed since their influence on other parameters is carried by the estimates and covariances of the station coordinates and Earth rotation parameters (see proof in Appendix C).

The quasi-observations from all of the GPS surveys were combined, estimating a consistent set of coordinates and velocities, with co-seismic displacements being estimated implicitly. We defined a reference frame by setting the a priori values of the coordinates and velocities of 8 stations (i.e., Algonquin, Ft. Davis, Kokee, Mojave, Pietown, Richmond, Yarragadee and Yellowknife; see Table 2.4 of *Bennett [1995]*) to those given by *Feigl et al. [1993]* from the combination of GPS and VLBI results, and applied constraints of 10 cm to the horizontal coordinates, 20 cm to the vertical coordinates, 1 mm/yr to the horizontal velocities, and 10 mm/yr to the vertical velocities. We applied loose a priori constraints to the coordinates (10 m) and velocities (200 mm/yr) of all other stations. In order to avoid corruption of the horizontal velocity field from large errors in vertical components due to incorrectly recorded heights and unmodeled phase-center variations of the antennas, we allowed a $0.04 \text{ m}^2/\text{yr}$ stochastic variation in the vertical coordinates of all of the stations. Constraints of 30 mas, 0.5 mas, and 1 m were assigned to network equatorial rotation, network axial rotation, and network center translation respectively (see equation (4) for definitions). We allowed the network to rotate and translate freely between non-adjacent experiments by assigning $3000 \text{ mas}^2/\text{yr}$, $0.5 \text{ mas}^2/\text{yr}$, and $300 \text{ m}^2/\text{yr}$ stochastic perturbations to equatorial rotation pole, axial rotation pole, and network center translation respectively. Larger a priori constraints and perturbation about the polar axis are unnecessary since the axial rotational variations are effectively absorbed by the looser constraints on orbital parameters.

After new quasi-observation data entered the Kalman filter and the parameter adjustments were updated, we transformed the coordinate and velocity adjustments from Cartesian to geodetic representation, and tested the compatibilities of the horizontal coordinate and velocity adjustments (2-dimensional), and vertical coordinate and velocity adjustments (1-

dimensional) separately. Incompatibility criteria were set at the 95% confidence level for horizontal components (2.45σ) and vertical components (2σ) after multiplying the formal uncertainties by a factor of two, as discussed above. Most data sets appeared compatible from the initial run but some incompatibilities remained. After inflating the covariance matrices of TREX18, IC93 Ashtech subset, and IC93 PGGA subset quasi-observations by additional factors of $(1.5)^2$, $(2.0)^2$, and $(2.0)^2$, all incompatibilities disappeared. We suspect that the incompatibilities for these two surveys result from the combination of subnets in which the overlapping stations were analyzed inconsistently or introduced errors due to unmodeled antenna phase-center variations. The compatibility of all of the surveys is indicated by the chi-square increments from the forward and backward filters, shown in Table 1 after the rescaling has been applied to TREX18 and IC93 but without the factor of two rescaling of the original quasi-observations. A total of 1188 quasi-observations were used to estimate 691 parameters at 114 stations. Our constraints reduced the parameter dimension by 112.64 and the stochastic perturbations increased it by 144.36. Thus the total degree of freedom was 466.28 and the postfit nrms was 1.82.

The GPS velocity solution is shown in Figure 3 with respect to a reference frame fixed to the North American plate. Our solution is statistically consistent with the earlier work of *Feigl et al.* [1993] and *Bennett* [1995] who used a similar approach and software but did not downweight the data from TREX18 and IC93. The net effect of our reweighting is to reduce the overall chi-square and improve the uncertainties for stations not heavily dependent on these two surveys. We have included 15 stations (AGUA, ALAM, ANZA, EDOM, INDO, JUR3, PSAR, RIAL, ROSA, RYAN, SAN1, SIPH, THOU, TRAN, and VIEW) which have large uncertainties from the GPS analysis but may be improved by a combination with the EDM if there are nearby EDM stations.

(c) EDM/GPS Combination

In the final step of our analysis, we combine the GPS derived velocity solution with the EDM-derived velocity solution. Since the scale difference between the EDM and GPS measurements is not completely resolved yet, we do not directly combine the EDM and GPS derived coordinate solutions to avoid biasing due to the unknown systematic differences [*Savage et al.*, 1996]. For the GPS derived velocity solution, we extract the velocity estimates and their sub-covariance matrix at 73 regional stations with redundant stations removed (e.g., stations close enough together that their velocities were equated in the solution). This suppression of parameters has no affect on the solution (see Appendix C) but greatly reduces the computational burden. For the EDM derived solution, we also removed the velocity

estimates for stations that are redundant or have weak estimates. In the combination, we rescaled the covariances of the GPS and EDM quasi-observations by factors of $(1.82)^2$ and $(1.22)^2$ respectively to make their nrms close to unity. To avoid introducing extra information in the combination, we assigned 10 m/yr a priori uncertainties for velocities of all stations. We tied the two data sets by forcing the horizontal velocities at the following station pairs to be equal (upper case is GPS; lower case is EDM): PIN1 and asbestos, NIGU and niguel, MONU and monu_res, BERD and berdoe, O225 and off_225, VIEW and view, TRAN and salton, SIPH and coach, OCOT and dixie, EDOM and edom. The observation number is 370.70 computed from the data contributed resolution matrices. The number of estimated parameters is 480. Constraints reduce the parameter dimension by 123.40, yielding 14.1 for the number of degrees of freedom of the combination solution. The nrms is 0.84, indicating that the GPS and EDM velocity quasi-observations are compatible and that our defined postfit χ^2 and degrees of freedom are self-consistent.

The GPS/EDM combined velocity field is plotted in Figure 4. This combined velocity solution passed our compatibility test. Comparison of Figure 3 with Figure 4 shows that the combination of the GPS and EDM velocity solutions not only densifies the derived velocity field, but also strengthens the estimates for many of the stations. The network orientation at the EDM stations is defined by the constrained velocity vectors at strong GPS stations such as PIN1, MONU, and NIGU. The value of these constraints is best illustrated by the large rotational uncertainties that remain for stations in the northern part of the Joshua-Anza network, which has only EDM stations. Similarly, the EDM measurements have reduced significantly the velocity uncertainties of the 5 stations that were weak from GPS measurements alone.

In Figure 5 we show an enlargement of the GPS-only and combined velocity fields for a 70-km square region spanning the San Andreas fault. In the combined solution (Figure 5b) the velocities of the GPS stations at EDOM, VIEW, PIN1, BERD, TRAN, and SIPH have been equated to nearby EDM stations and show considerable improvement compared with GPS alone (Figure 5a). The well-determined velocities at GPS station PAIN are not equated to the velocities at nearby EDM station mecca and hence show the consistency of the two data sets. The elongated ellipse belongs to the two VIEW velocities (coincident in the plot), demonstrating that the GPS determined weak velocity estimate at VIEW has been improved only in one direction because the EDM station view has only single baseline measurements connected to the EDM network. In order to show the one-direction improvement at VIEW, we did not equate the velocity estimate at VIEW with the velocity estimate at a nearby EDM

station (inspencer) whose velocity is consistent with VIEW and is well determined in the north-south direction.

8. Conclusions

A combination of space and terrestrial geodetic data effectively strengthens the velocity solution. The quasi-observation approach provides greater flexibility and efficiency in combining various types of geodetic measurements without losing tectonic information. These quasi-observations are obtained by analyzing primary data using loose constraints. Loose constraints are necessary to minimize the inconsistencies between different data sets and between different types of geodetic measurements. Only in the final combination stage is a homogeneous reference system established by tightly constraining coordinates and/or velocities at several stations. Such an approach also makes some weak data (such as STRC88) useful for the deformation analysis since the local stations can be strengthened by later strong data under a homogeneous reference frame therefore improving originally poorly-determined orbits. However, the quasi-observation approach also raises some unresolved problems, in particular for the statistics. We have developed useful tools to determine the increment of postfit χ^2 , to perform a compatibility test for a combined solution when both data and parameters are added, and to calculate an appropriate degree of freedom and nrms when both constraints and perturbations are applied. Note that the deformation analysis is a very broad area which can not be covered by a single paper. Some important issues, such as the optimal quasi-observation data reweighting, the colored noise model rather than white noise model in data analysis, and the time-dependent deformation such as the post-seismic deformation, are not discussed in this paper. Furthermore, the geodetic quasi-observation data combination is not yet fully covered by a rigorous statistics theory so that many investigators including this study must use some empirical rules to reach a resolution. The example presented in this study is a good example for addressing the importance of adopting appropriate constraints, compatibility test and reasonable statistics, but not for a velocity field. A more reliable velocity field in this region should be derived using the reanalyzed GPS quasi-observations to reduce some significant problems such as the ill-conditioned covariance matrices. Although the method presented in this paper is primarily used to estimate a regional horizontal deformation field from a combination of geodetic data, it can be easily extended to estimate a vertical deformation field by incorporating leveling and gravity observations.

Appendix A

Linearized observation equations for various primary observations

We present all estimated parameters in the geocentric Cartesian frame. Detailed derivations of these linearized equations can be found in *King et al.* [1985] for GPS measurements, in *Herring* [1983] for VLBI measurements and in *Collier et al.* [1988] for terrestrial survey measurements. In analyzing primary observations, we estimate only the time-dependent station positions $\Delta\mathbf{X}(\mathbf{a},t)$ (simplified as $\delta\mathbf{X}$ in this section) and reparameterize the time-dependent station positions $\Delta\mathbf{X}(\mathbf{a},t)$ by (4) at the next combination step.

1) *Baseline and baseline rate vectors in geocentric Cartesian frame:*

$$\delta(d\mathbf{X}_{ij}) = \delta\mathbf{X}_j - \delta\mathbf{X}_i, \quad \delta(d\mathbf{V}_{ij}) = \delta\mathbf{V}_{0j} - \delta\mathbf{V}_{0i} \quad (\text{A.1})$$

2) *Astronomic longitude Λ , latitude Φ , and gravity g :*

$$\begin{pmatrix} \delta\Lambda \\ \delta\Phi \\ \delta g \end{pmatrix} = - \begin{pmatrix} (g_0 \cos \phi_0)^{-1} & 0 & 0 \\ 0 & g_0^{-1} & 0 \\ 0 & 0 & 1 \end{pmatrix} \mathbf{R}_0 \left(\mathbf{M} \delta\mathbf{X} + \frac{\partial(\Delta U_0(\mathbf{X}_0))}{\partial \mathbf{X}} \right) \quad (\text{A.2})$$

where

g_0 is the a priori gravity, ϕ_0 is the a priori geodetic latitude, and

$$\mathbf{M} = \frac{\partial^2 U}{\partial \mathbf{X}^2}$$

is the Marussi tensor of second-order derivatives of U [*Hein*, 1986].

\mathbf{R}_0 is defined by

$$\mathbf{R}(t) = \begin{bmatrix} -\sin \Lambda(t) & \cos \Lambda(t) & 0 \\ -\sin \Phi(t) \cos \Lambda(t) & -\sin \Phi(t) \sin \Lambda(t) & \cos \Phi(t) \\ \cos \Phi(t) \cos \Lambda(t) & \cos \Phi(t) \sin \Lambda(t) & \sin \Phi(t) \end{bmatrix} \quad (\text{A.3})$$

with the a priori astronomic latitude Φ_0 and longitude Λ_0 .

If the disturbing potential ΔU_0 is dominated by known mass anomalies, then the ΔU_0 term in (A.2) represents the deflections of the vertical for astronomical latitude and longitude Λ and Φ , and the topographic gravity anomaly [*Hein*, 1986]. We impose the corrections of the deflections of the vertical and the topographic gravity anomaly in advance, so that (A.2) becomes

$$\begin{pmatrix} \delta\Lambda \\ \delta\Phi \\ \delta g \end{pmatrix} = - \begin{pmatrix} (g_0 \cos \phi_0)^{-1} & 0 & 0 \\ 0 & g_0^{-1} & 0 \\ 0 & 0 & 1 \end{pmatrix} R_0 M \delta X \quad (\text{A.4})$$

3) Horizontal and vertical angles and mark-to-mark distances

From local station i to station j , the distance is $l(t)$, the azimuth is $\alpha(t)$, and the vertical angle is $\beta(t)$. The linearized observation equations of triangulation, leveling, and trilateration are expressed as:

$$\begin{pmatrix} \delta\alpha \\ \delta\beta \\ \delta l \end{pmatrix} = \begin{pmatrix} (l_0 \cos \beta_0)^{-1} & 0 & 0 \\ 0 & l_0^{-1} & 0 \\ 0 & 0 & 1 \end{pmatrix} \left[S^T R_0 (\delta X_j - \delta X_i) - \frac{K R_0 M}{g_0} \delta X_i \right] \quad (\text{A.5})$$

where

$$S = \begin{pmatrix} \cos \alpha_0 & -\sin \alpha_0 \sin \beta_0 & \sin \alpha_0 \cos \beta_0 \\ -\sin \alpha_0 & -\cos \alpha_0 \sin \beta_0 & \cos \alpha_0 \cos \beta_0 \\ 0 & \cos \beta_0 & \sin \beta_0 \end{pmatrix} \quad (\text{A.6})$$

$$K = \begin{pmatrix} l_0 (\tan \phi_0 \cos \beta_0 - \cos \alpha_0 \sin \beta_0) & l_0 \sin \alpha_0 \sin \beta_0 & 0 \\ l_0 \sin \alpha_0 & l_0 \cos \alpha_0 & 0 \\ 0 & 0 & 0 \end{pmatrix} \quad (\text{A.7})$$

and the zero subscript indicates values calculated from a priori coordinates.

As mentioned before, the left-side terms of (A.5) have included the corrections for the deflection of the vertical. For direction observations, we adopt auxiliary parameters to account for the unknown arbitrary azimuth of the first "pointing" in each "zero". This approach is equivalent to the angle difference method, but the latter must construct a full, rather than a diagonal, covariance matrix to describe the correlations among observations [Prescott, 1976].

4) GPS carrier beat phase

$$\delta\phi_i(t) = -\frac{f_i}{c} |\delta X(t) - \delta X^s(t)| + \delta\phi_i^{t+c}(t) + \frac{\kappa(t)}{f_i} + b_i \quad (\text{A.10})$$

where

$i = 1, 2$ corresponding to two carrier frequencies f_1, f_2 ,

$\delta\phi_i$ are carrier beat phases,

t is the receiver time, c is the speed of light,

$\delta X(t)$ and $\delta X^s(t)$ are time-dependent station and satellite positions,

$\delta\phi_i^{t+c}$ are phases from tropospheric delay, transmitter and receiver oscillator,
 κ is ionosphere refraction variable,
 b_i are mixture of ambiguity and initial phase offset

5) Range to a satellite

$$\delta\rho(t) = |\delta\mathbf{X}(t) - \delta\mathbf{X}^s(t)| + \delta\rho^p(t) \quad (\text{A.11})$$

where

$\delta\rho(t)$ is the range from receiver to satellite,

$\delta\mathbf{X}(t)$ and $\delta\mathbf{X}^s(t)$ are time-dependent station and satellite positions,

$\delta\rho^p(t)$ is the range from various perturbation sources to which the observable is sensitive, such as geopotential model, tidal model, drag and solar radiation pressure models, Earth rotation parameters, *etc.*

6) VLBI group delay

$$\delta\tau(t) = -\frac{\delta(d\mathbf{X}_{ij}(t)) \cdot \mathbf{e}_s}{c} + \delta\tau^p(t) \quad (\text{A.12})$$

where

$\delta\tau(t)$ is the group delay observable,

$\delta\mathbf{X}_{ij}(t)$ is the baseline vector,

\mathbf{e}_s is a unit vector towards the radio source, c is the speed of light,

$\delta\tau^p(t)$ is the group delay from various perturbation sources to which the observable is sensitive, such as troposphere and ionosphere delay models, nutation model, radio source structure parameters, *etc.*

Appendix B:

Sum of the squared residuals (χ^2)

In the case of time-invariant parameters and without state perturbation, our definition of (13) becomes

$$\chi_{k+1}^2 - \chi_k^2 = (\delta\mathbf{l}_{k+1} - \mathbf{A}_{k+1} \delta\hat{\mathbf{x}}_{k+1})^T \mathbf{P}_{k+1}^{-1} (\delta\mathbf{l}_{k+1} - \mathbf{A}_{k+1} \delta\hat{\mathbf{x}}_{k+1}) + \Delta\hat{\mathbf{x}}_{k+1}^T \mathbf{C}_k^{-1} \Delta\hat{\mathbf{x}}_{k+1} \quad (\text{B.1})$$

$$\text{Where } \Delta\hat{\mathbf{x}}_{k+1} = \delta\hat{\mathbf{x}}_{k+1} - \delta\hat{\mathbf{x}}_k \quad (\text{B.2})$$

$$\delta\hat{\mathbf{x}}_k = \mathbf{C}_k \mathbf{A}_k^T \mathbf{P}_k^{-1} \delta\mathbf{l}_k \quad (\text{B.3a})$$

$$\mathbf{C}_k = (\mathbf{A}_k^T \mathbf{P}_k^{-1} \mathbf{A}_k)^{-1} \quad (\text{B.3b})$$

$$\chi_k^2 = (\delta\mathbf{l}_k - \mathbf{A}_k \hat{\mathbf{x}}_k)^T \mathbf{P}_k^{-1} (\delta\mathbf{l}_k - \mathbf{A}_k \hat{\mathbf{x}}_k) \quad (\text{B.3c})$$

In (B.3c) $\delta\mathbf{l}_k$ represents observation vector from t_1 to t_k . Thus (B.3c) represents the sum of squared residuals from t_1 to t_k .

By adding observation $\delta \mathbf{l}_{k+1} = \mathbf{A}_{k+1} \delta \mathbf{x} + \boldsymbol{\varepsilon}_{k+1}$ at t_{k+1} , the least squares solutions for all observations are

$$\begin{aligned} \delta \widehat{\mathbf{x}}_{k+1} &= \mathbf{C}_{k+1} (\mathbf{A}_k^T \mathbf{P}_k^{-1} \delta \mathbf{l}_k + \mathbf{A}_{k+1}^T \mathbf{P}_{k+1}^{-1} \delta \mathbf{l}_{k+1}) \\ &= \delta \widehat{\mathbf{x}}_k + \mathbf{C}_k \mathbf{A}_{k+1}^T (\mathbf{P}_{k+1}^{-1} + \mathbf{A}_{k+1} \mathbf{C}_k \mathbf{A}_{k+1}^T)^{-1} (\delta \mathbf{l}_{k+1} - \mathbf{A}_{k+1} \delta \widehat{\mathbf{x}}_k) \end{aligned} \quad (\text{B.4a})$$

$$\mathbf{C}_{k+1} = (\mathbf{A}_k^T \mathbf{P}_k^{-1} \mathbf{A}_k + \mathbf{A}_{k+1}^T \mathbf{P}_{k+1}^{-1} \mathbf{A}_{k+1})^{-1} \quad (\text{B.4b})$$

$$\chi_{k+1}^2 = (\delta \mathbf{l}_k - \mathbf{A}_k \delta \widehat{\mathbf{x}}_{k+1})^T \mathbf{P}_k^{-1} (\delta \mathbf{l}_k - \mathbf{A}_k \delta \widehat{\mathbf{x}}_{k+1}) + (\delta \mathbf{l}_{k+1} - \mathbf{A}_{k+1} \delta \widehat{\mathbf{x}}_{k+1})^T \mathbf{P}_{k+1}^{-1} (\delta \mathbf{l}_{k+1} - \mathbf{A}_{k+1} \delta \widehat{\mathbf{x}}_{k+1}) \quad (\text{B.4c})$$

Using (B.2) and (B.3c), we get

$$\begin{aligned} (\delta \mathbf{l}_k - \mathbf{A}_k \delta \widehat{\mathbf{x}}_{k+1})^T \mathbf{P}_k^{-1} (\delta \mathbf{l}_k - \mathbf{A}_k \delta \widehat{\mathbf{x}}_{k+1}) &= \chi_k^2 + \Delta \widehat{\mathbf{x}}_{k+1}^T \mathbf{A}_k^T \mathbf{P}_k^{-1} \mathbf{A}_k \Delta \widehat{\mathbf{x}}_{k+1} \\ &\quad - (\delta \mathbf{l}_k - \mathbf{A}_k \delta \widehat{\mathbf{x}}_k)^T \mathbf{P}_k^{-1} \mathbf{A}_k \Delta \widehat{\mathbf{x}}_{k+1} - \Delta \widehat{\mathbf{x}}_{k+1}^T \mathbf{A}_k^T \mathbf{P}_k^{-1} (\delta \mathbf{l}_k - \mathbf{A}_k \delta \widehat{\mathbf{x}}_k) \end{aligned} \quad (\text{B.5a})$$

(B.3a) and (B.3b) imply

$$(\delta \mathbf{l}_k - \mathbf{A}_k \delta \widehat{\mathbf{x}}_k)^T \mathbf{P}_k^{-1} \mathbf{A}_k = \mathbf{A}_k^T \mathbf{P}_k^{-1} (\delta \mathbf{l}_k - \mathbf{A}_k \delta \widehat{\mathbf{x}}_k) = 0 \quad (\text{B.5b})$$

Substituting (B.3b), (B.5a) and (B.5b) for (B.4c), we get (B.1). Thus, we proved that in the case of time-invariant parameters and without state perturbation, our definition (13) is equivalent to the classical definition of χ^2 .

The Kalman gain can be written in another useful form

$$\mathbf{K}_{k+1} = (\mathbf{C}_{k+1|k}^{-1} + \mathbf{A}_{k+1}^T \mathbf{P}_{k+1}^{-1} \mathbf{A}_{k+1})^{-1} \mathbf{A}_{k+1}^T \mathbf{P}_{k+1}^{-1} \quad (\text{B.6})$$

Substituting (B.6) for (11b), we have

$$\mathbf{C}_{k+1}^{-1} = \mathbf{C}_{k+1|k}^{-1} + \mathbf{A}_{k+1}^T \mathbf{P}_{k+1}^{-1} \mathbf{A}_{k+1} \quad (\text{B.7})$$

This is just the standard weighted least-squares increment to the information matrix. (B.6), (B.7) and (11a) give

$$\Delta \widehat{\mathbf{x}}_{k+1} = \mathbf{C}_{k+1|k} \mathbf{A}_{k+1}^T \mathbf{P}_{k+1}^{-1} (\delta \mathbf{l}_{k+1} - \mathbf{A}_{k+1} \delta \mathbf{x}_{k+1}) \quad (\text{B.8})$$

Using (11a) and (12), we also get

$$\delta \mathbf{l}_{k+1} - \mathbf{A}_{k+1} \delta \widehat{\mathbf{x}}_{k+1} = \mathbf{P}_{k+1} (\mathbf{P}_{k+1} + \mathbf{A}_{k+1} \mathbf{C}_{k+1|k} \mathbf{A}_{k+1}^T)^{-1} (\delta \mathbf{l}_{k+1} - \mathbf{A}_{k+1} \delta \widehat{\mathbf{x}}_{k+1|k}) \quad (\text{B.9})$$

Substituting (B.8), (B.9) for (13), we obtain (15)

Appendix C

Reparameterization

Let x and y be two different parameterizations of the same observations l ,

$$l = \mathbf{A}_x x + \boldsymbol{\varepsilon}_x \quad \text{with covariance } \mathbf{C}_l \quad (\text{C.1})$$

$$l = \mathbf{A}_y y + \boldsymbol{\varepsilon}_y \quad \text{with covariance } \mathbf{C}_l \quad (\text{C.2})$$

Assuming the dimensions for l , x , y are n , m_x , m_y ($n \geq m_y \geq m_x$) respectively, and $\boldsymbol{\varepsilon}_x$, $\boldsymbol{\varepsilon}_y$ are Gaussian, the least square estimates are well known:

$$\hat{x} = (A_x^T C_l^{-1} A_x)^{-1} A_x^T C_l^{-1} l \quad (C.3)$$

$$C_{\hat{x}} = (A_x^T C_l^{-1} A_x)^{-1} \quad (C.4)$$

$$\hat{y} = (A_y^T C_l^{-1} A_y)^{-1} A_y^T C_l^{-1} l \quad (C.5)$$

$$C_{\hat{y}} = (A_y^T C_l^{-1} A_y)^{-1} \quad (C.6)$$

The weighted sums of squared residuals (χ^2) are

$$\chi_x^2 = (l - A_x \hat{x})^T C_l^{-1} (l - A_x \hat{x}) = l^T C_l^{-1} l - l^T C_l^{-1} A_x C_{\hat{x}} A_x^T C_l^{-1} l \quad (C.7)$$

$$\chi_y^2 = (l - A_y \hat{y})^T C_l^{-1} (l - A_y \hat{y}) = l^T C_l^{-1} l - l^T C_l^{-1} A_y C_{\hat{y}} A_y^T C_l^{-1} l \quad (C.8)$$

Both χ_x^2 and χ_y^2 obey χ^2 - distribution with $n-m_x$, $n-m_y$ degrees of freedom respectively.

1) Use \hat{y} and $C_{\hat{y}}$ as quasi-observations to estimate x

It is easy to prove that if we construct a quasi-observation equation

$$\hat{y} = B x \quad \text{with covariance matrix } C_{\hat{y}} \quad (C.9)$$

the solution is:

$$\hat{x} = (B^T C_{\hat{y}}^{-1} B)^{-1} B^T C_{\hat{y}}^{-1} \hat{y} = (3.3) \quad (C.10)$$

$$C_{\hat{x}} = (B^T C_{\hat{y}}^{-1} B)^{-1} = (3.4) \quad (C.11)$$

$$\chi^2 = (\hat{y} - B\hat{x})^T C_{\hat{y}}^{-1} (\hat{y} - B\hat{x}) = \chi_x^2 - \chi_y^2 \quad (C.12)$$

The χ^2 also obey χ^2 - distribution with $m_y - m_x$ degrees of freedom. In most practical cases, the information of n and χ_y^2 is lost in the quasi-observation data files. Thus, the statistics of χ^2 is in general not the same as the statistics of χ_x^2 unless $n \gg m_y \gg m_x$ and $\frac{\chi_x^2}{n - m_x}$, $\frac{\chi_y^2}{n - m_y}$ have the same expectation, such a case is usually not valid in the deformation analysis because the error spectrum (the long term error vs. the short term error) is more likely not flat.

2) Use \hat{y} and $C_{\hat{y}}$ as quasi-observations and add extra parameters x_a to x

The quasi-observation equation is

$$y = (B_x \quad B_{x_a}) \begin{pmatrix} x \\ x_a \end{pmatrix} \quad (C.13)$$

To distinguish from (C.10) and (C.11), we use \tilde{x} and $C_{\tilde{x}}$ to denote the estimated subsolutions of (C.13). After some manipulations, we obtain the relations

$$\tilde{x} = \hat{x} + Q_{12} Q_{22}^{-1} \tilde{x}_a \quad (C.14)$$

$$C_{\tilde{x}} = C_{\hat{x}} + Q_{12} Q_{22}^{-1} Q_{21} \quad (C.15)$$

where

$$C_{\hat{x}} = N_{11}^{-1}, \quad C_{\tilde{x}} = Q_{11}, \quad Q_{12} = -N_{11}^{-1} N_{12} Q_{22} = Q_{21}^T$$

$$N_{12} = A_x^T C_l^{-1} A_{x_a}, \quad N_{22} = A_{x_a}^T C_l^{-1} A_{x_a}, \quad A_{x_a} = A_y B_{x_a} \quad (C.16)$$

$$Q_{22} = (N_{22} - N_{21} N_{11}^{-1} N_{12})^{-1} = C_{\tilde{x}_a}$$

From (C.11), it is straightforward to get

$$C_{\tilde{x}-\hat{x}} = Q_{12} Q_{22}^{-1} Q_{21} \quad (C.17)$$

Then

$$C_{\tilde{x}} = C_{\hat{x}} + C_{\tilde{x}-\hat{x}} \quad (C.18)$$

If the parameters x_a actually do not exist, the expectation of the observation is

$$E\{l\} = A_x \bar{x} \quad (C.19)$$

From (C.16) and using (C.19)

$$\begin{aligned} E\{\tilde{x}\} &= E\{\hat{x}\} + Q_{12} Q_{22}^{-1} (Q_{21} A_x^T C_1^{-1} + Q_{22} A_{x_a}^T C_1^{-1}) E\{l\} \\ &= \bar{x} + Q_{12} Q_{22}^{-1} (Q_{21} N_{11} + Q_{22} N_{21}) \bar{x} = \bar{x} \end{aligned} \quad (C.20)$$

If the additional parameters x_a do not exist, \tilde{x} is still an unbiased estimate of x , but its covariance is enlarged (see (C.18)). On the other hand, if the additional parameters x_a do exist, the omission of x_a will underestimate the variance of x and lead to a biased estimate \tilde{x} unless the expectation of x_a is zero.

3) Two data sets related to two sets of parameters with only part of the parameters in common

Assume the first data set is related to parameters x_1 and x_2 and the second data set is related to parameters x_2 and x_3 . The typical example is to consider space geodetic data as the first data set and terrestrial survey data as the second data set. In this case the quasi-observation equations are

$$\begin{pmatrix} \hat{x}_1 \\ \hat{x}_2 \end{pmatrix} = \begin{pmatrix} I & 0 \\ 0 & E_2 \end{pmatrix} \begin{pmatrix} x_1 \\ x_2 \end{pmatrix} \quad \text{with covariance matrix } C = \begin{pmatrix} C_{11} & C_{12} \\ C_{21} & C_{22} \end{pmatrix} \quad (C.21)$$

The combined normal equations are

$$\begin{pmatrix} N_{11} & N_{12}E_2 & 0 \\ E_2^T N_{21} & E_2^T N_{22}E_2 + A_{22} & A_{23} \\ 0 & A_{32} & A_{33} \end{pmatrix} \begin{pmatrix} x_1 \\ x_2 \\ x_3 \end{pmatrix} = \begin{pmatrix} N_{11}\hat{x}_1 + N_{12}\hat{x}_2 \\ B_2 + E_2^T N_{21}\hat{x}_1 + E_2^T N_{22}\hat{x}_2 \\ B_3 \end{pmatrix} \quad (C.22)$$

Here $N = C^{-1}$.

Solving x_1 implicitly and using the matrix partition formula, we obtain

$$\begin{pmatrix} E_2^T C_{22}^{-1} E_2 + A_{22} & A_{23} \\ A_{32} & A_{33} \end{pmatrix} \begin{pmatrix} x_2 \\ x_3 \end{pmatrix} = \begin{pmatrix} B_2 + E_2^T C_{22}^{-1} \hat{x}_2 \\ B_3 \end{pmatrix} \quad (C.23)$$

This important result shows that if we do not care about the estimate of x_1 , we can use only the common parameters x_2 and their covariance submatrix C_{22} as the quasi-observations. The result is as rigorous as using all parameters.

4) Use part of the solutions to estimate another set of parameters

Assuming the solutions include parameters x_1 and x_2 , we attempt to use x_2 to estimate another parameter set u_2 . A typical example is to estimate fault slips (u_2) from episodic station displacement estimates (\hat{x}_2).

$$\begin{pmatrix} \hat{x}_1 \\ \hat{x}_2 \end{pmatrix} = \begin{pmatrix} I & 0 \\ 0 & E_2 \end{pmatrix} \begin{pmatrix} x_1 \\ u_2 \end{pmatrix} \quad \text{with covariance matrix } C = \begin{pmatrix} C_{11} & C_{12} \\ C_{21} & C_{22} \end{pmatrix} \quad (\text{C.24})$$

As has been proved above, using \hat{x}_2 and its covariance submatrix C_{22} as the quasi-observations, we can obtain the same estimates directly by estimating x_1 and u_2 from the raw data. Since the episodic station displacements better describe the real coseismic deformation field than the fault slip parameters, such an approach enables us to leave the model errors in the residuals without distorting the original estimate of \hat{x}_1 .

Appendix D

Solution changes in the case of adding new data and new parameters

It is instructive to first look at the classical case of time-invariant parameters and without state perturbation. Assume the original data l_1 relate to the parameters x , and the new data l_2 relate to parameters x and y . \hat{x}_1 are the original estimate and $\hat{x}_{1+2}, \hat{y}_{1+2}$ are estimates from data l_1+l_2 .

$$l_1 = A_1 x + \varepsilon_1 \quad \text{with covariance } C_{11} \quad (\text{D.1})$$

$$l_2 = B_1 x + B_2 y + \varepsilon_2 \quad \text{with covariance } C_{12} \quad (\text{D.2})$$

The covariance matrices are

$$C_{\hat{x}_1} = (A_1^T C_{11}^{-1} A_1)^{-1} \quad (\text{D.3})$$

$$C_{\begin{pmatrix} \hat{x}_{1+2} \\ \hat{y}_{1+2} \end{pmatrix}} = \begin{pmatrix} A_1^T C_{11}^{-1} A_1 + B_1^T C_{12}^{-1} B_1 & B_1^T C_{12}^{-1} B_2 \\ B_2^T C_{12}^{-1} B_1 & B_2^T C_{12}^{-1} B_2 \end{pmatrix}^{-1} = \begin{pmatrix} N_{11} & N_{12} \\ N_{21} & N_{22} \end{pmatrix}^{-1} = \begin{pmatrix} Q_{11} & Q_{12} \\ Q_{21} & Q_{22} \end{pmatrix} \quad (\text{D.4})$$

$$C_{\hat{x}_{1+2}} = Q_{11} \quad (\text{D.5})$$

The solution change of parameters x can be derived as

$$\hat{x}_{1+2} - \hat{x}_1 = (Q_{11} - (A_1^T C_{11}^{-1} A_1)^{-1}) A_1^T C_{11}^{-1} l_1 + (Q_{11} B_1^T + Q_{12} B_2^T) C_{12}^{-1} l_2 \quad (\text{D.6})$$

Since the two data sets are uncorrelated,

$$\begin{aligned} C_{\hat{x}_{1+2} - \hat{x}_1} &= (Q_{11} - (A_1^T C_{11}^{-1} A_1)^{-1}) A_1^T C_{11}^{-1} A_1 (Q_{11} - (A_1^T C_{11}^{-1} A_1)^{-1}) + (Q_{11} B_1^T + Q_{12} B_2^T) C_{12}^{-1} (B_1 Q_{11} + B_2 Q_{21}) \\ &= (Q_{11} N_{11} + Q_{12} N_{21} - I) Q_{11} - Q_{11} + C_{\hat{x}_1} + (Q_{11} N_{12} + Q_{12} N_{22}) Q_{21} \end{aligned}$$

From the well-known relations,

$$Q_{11} N_{11} + Q_{12} N_{21} = I \quad \text{and} \quad Q_{11} N_{12} + Q_{12} N_{22} = 0$$

We derive the very simple result

$$C_{\hat{x}_{1+2} - \hat{x}_1} = C_{\hat{x}_1} - C_{\hat{x}_{1+2}} \quad (\text{D.7})$$

In the general case of allowing time-variant parameters and state perturbation, the Kalman filtering formulation gives (see (11a))

$$\delta\hat{\mathbf{x}}_{k+1} - \delta\hat{\mathbf{x}}_{k+1|k} = \mathbf{K}_{k+1} (\delta\mathbf{l}_{k+1} - \mathbf{A}_{k+1} \delta\hat{\mathbf{x}}_{k+1|k}) \quad (\text{D.8})$$

Note that $\delta\mathbf{l}_{k+1}$ and $\delta\hat{\mathbf{x}}_{k+1|k}$ are uncorrelated, therefore

$$\mathbf{C}_{\hat{\mathbf{x}}_{k+1} - \hat{\mathbf{x}}_{k+1|k}} = \mathbf{K}_{k+1} \mathbf{P}_{k+1} \mathbf{K}_{k+1}^T + \mathbf{K}_{k+1} \mathbf{A}_{k+1} \mathbf{C}_{k+1|k} \mathbf{A}_{k+1}^T \mathbf{K}_{k+1}^T \quad (\text{D.9})$$

From (12),

$$\begin{aligned} \mathbf{K}_{k+1} \mathbf{A}_{k+1} \mathbf{C}_{k+1|k} \mathbf{A}_{k+1}^T &= \mathbf{K}_{k+1} (\mathbf{A}_{k+1} \mathbf{C}_{k+1|k} \mathbf{A}_{k+1}^T + \mathbf{P}_{k+1} - \mathbf{P}_{k+1}) \\ &= \mathbf{C}_{k+1|k} \mathbf{A}_{k+1}^T - \mathbf{K}_{k+1} \mathbf{P}_{k+1} \end{aligned}$$

Thus (D.9) is reduced to

$$\mathbf{C}_{\hat{\mathbf{x}}_{k+1} - \hat{\mathbf{x}}_{k+1|k}} = \mathbf{C}_{k+1|k} \mathbf{A}_{k+1}^T \mathbf{K}_{k+1}^T \quad (\text{D.10})$$

Replacing the right hand term of (D.10) by (11b), we get

$$\mathbf{C}_{\hat{\mathbf{x}}_{k+1} - \hat{\mathbf{x}}_{k+1|k}} = \mathbf{C}_{k+1|k} - \mathbf{C}_{k+1} \quad (\text{D.11})$$

Such a relation can be extended to the backward filter with the Gelb's weighted mean smoothing algorithm [see *Herring et al.*, 1990 for details]. Let $\delta\hat{\mathbf{x}}_{k+1}$ and \mathbf{C}_{k+1} represent the forward filtering solution and covariance matrix at epoch $k+1$, $\delta\hat{\mathbf{x}}_{k+1|k}$ and $\mathbf{C}_{k+1|k}$ represent the predicted solution and covariance matrix at epoch $k+1$ from the forward filtering solution at epoch k , $\delta\hat{\mathbf{x}}_{k+1|k+2}$ and $\mathbf{C}_{k+1|k+2}$ represent the predicted solution and covariance matrix at epoch $k+1$ from the backward filtering solution at epoch $k+2$. The smoothing solution and its covariance matrix will be

$$\delta\hat{\mathbf{x}}_{k+1}^s = \delta\hat{\mathbf{x}}_{k+1} + \mathbf{M} (\delta\hat{\mathbf{x}}_{k+1|k+2} - \delta\hat{\mathbf{x}}_{k+1}) \quad (\text{D.12})$$

$$\mathbf{C}_{k+1}^s = \mathbf{C}_{k+1} - \mathbf{M} \mathbf{C}_{k+1} \quad (\text{D.13})$$

where

$$\mathbf{M} = \mathbf{C}_{k+1} (\mathbf{C}_{k+1} + \mathbf{C}_{k+1|k+2})^{-1} \quad (\text{D.14})$$

Similarly, we can define another "smoothing" solution at epoch $k+1$ using all data except the data at epoch $k+1$:

$$\delta\hat{\mathbf{x}}_{k+1}^* = \delta\hat{\mathbf{x}}_{k+1|k} + \mathbf{M}^* (\delta\hat{\mathbf{x}}_{k+1|k+2} - \delta\hat{\mathbf{x}}_{k+1|k}) \quad (\text{D.15})$$

It can be proved that

$$\mathbf{C}_{k+1}^* = \mathbf{C}_{k+1|k} - \mathbf{M}^* \mathbf{C}_{k+1|k} \quad (\text{D.16})$$

where

$$\mathbf{M}^* = \mathbf{C}_{k+1|k} (\mathbf{C}_{k+1|k} + \mathbf{C}_{k+1|k+2})^{-1} \quad (\text{D.17})$$

Since $\delta\hat{\mathbf{x}}_{k+1}$ and $\delta\hat{\mathbf{x}}_{k+1|k}$ are uncorrelated with $\delta\hat{\mathbf{x}}_{k+1|k+2}$, direct manipulations lead to

$$\mathbf{C}_{\delta\hat{\mathbf{x}}_{k+1}^* - \delta\hat{\mathbf{x}}_{k+1}^s} = \mathbf{C}_{k+1}^* - \mathbf{C}_{k+1}^s \quad (\text{D.18})$$

Appendix E

System constraints

We parameterize the relation between the estimated coordinates from the loose analysis and the a priori coordinate system as

$$\hat{x}_n = x_a + \mathbf{T}\theta + \delta x_n \quad (\text{E.1})$$

where \hat{x}_n are the parameter estimates from the loose analysis, x_a are the a priori values of the parameters; θ are the transformation parameters; \mathbf{T} is the Jacobean relating the transformation parameters to the analysis parameters and δx_n are the residuals of the loose analysis after applying the transformation. The transformation parameters θ can consist of rotations, translations and scale parameters. The rows of \mathbf{T} corresponding to the parameters that are not station coordinate parameters are null. We now seek the estimates of θ which will minimize

$$\delta x_n \mathbf{W} \delta x_n^T \quad (\text{E.2})$$

where \mathbf{W} is a weight matrix. The weight matrix is formed such that the height coordinate is given less weight than the horizontal coordinates (usually 10 times less weight), and only selected stations are weighted in \mathbf{W} ; i.e., not all stations are used to estimate θ . The estimates of θ are obtained by conventional weighted least squares analysis, which we express in the form

$$\hat{\theta} = \mathbf{T}^- \Delta x_n = \left(\mathbf{T}^T \mathbf{W} \mathbf{T} \right)^{-1} \mathbf{T}^T \mathbf{W} \Delta x_n \quad (\text{E.3})$$

where \mathbf{T}^- is the generalized inverse of \mathbf{T} and $\Delta x_n = \hat{x}_n - x_a$.

The rank deficiencies of the system are removed by forcing the estimates of θ to have zero variance. From equations (11a) and (11b) we then have

$$\hat{x}_c = \hat{x}_n - \mathbf{K}_c \hat{\theta} \quad (\text{E.4a})$$

$$\mathbf{C}_c = \mathbf{C}_n - \mathbf{K}_c \mathbf{T}^- \mathbf{C}_n \quad (\text{E.4b})$$

where the constraint Kalman gain matrix is given by equation (12)

$$\mathbf{K}_c = \mathbf{C}_n \mathbf{T}^{-T} \left(\mathbf{T}^- \mathbf{C}_n \mathbf{T}^{-T} \right)^{-1} \quad (\text{E.5})$$

and C_n is the variance-covariance matrix of parameter estimates from the loose analysis, and we have reversed the sign of θ so that transformation parameters will be removed from the loose analysis results. (As given in Equation E.1, θ represents parameters to transform the a priori coordinates to the loose analysis results).

If the parameters in θ represent true rank deficiencies in the loose analysis or if $W^{-1} = C_n$, then $K_c = T$ and equation E.4b reduces the least squares definition of the variance-covariance matrix of the postfit residuals. We have confirmed the former numerically and the latter analytically. For the above cases, quantities that are invariant under the transformation T are not affected by applying the constraints nor are their variances. Specifically, if T represents only rotations and translations, then baseline lengths and their variances are not changed by the application of equation (E.4).

For VLBI measurements to extragalactic quasars, both translation and rotation are rank deficiencies and therefore θ should contain both types of parameters. For GPS, only rotation is a rank deficiency unless explicit parameters are added to the analysis that allow the coordinate system to translate. For neither system is the scale a rank deficiency although given the points noted above it might be prudent to include scale parameters in the analysis. Errors in the antenna phase patterns will cause all heights to be systematically biased, which will appear as a scale error.

In Figure E.1 we examine a specific example of the effects of applying coordinate system constraints in an analysis of GPS data from 80 global stations. The results in this figure are for the case when explicit translation and scale parameters are not included in the analysis. As a measure of the impact of the constraints we show the changes in baseline lengths when the constraints are applied. (If explicit translation and scale parameters are included then the changes in the baselines lengths are zero for the translation parameters and simply the scale change for the scale parameter). The figure shows the effects of separate 1 m translations in the X, Y and Z coordinates and a 160 parts-per-billion (ppb) scale change (equivalent to a 1 m height change for all stations). Since the constraints are a linear operator, the effects in Figure E.1 can be scaled in proportion to more realistic translations and scale change. From Figure E.1 it is clear that applying the constraint in Equation (E.4a) is not the same as simply translating or scaling the GPS results. This is particularly true for the scale change where the difference between a simple scaling and the constraint can be a factor of 5 times larger than the scale change itself. For the translations, the correlations between the position estimates does allow for changes in position that are more of a translational nature. Figure E.1 (a)-(c) pose an interesting question: are GPS results better when the coordinate estimates are forced

to the expected center of mass, or is it better to allow them to translate freely? The answer to this question depends on the quality of the a priori coordinates and how close they lie to the true, instantaneous center of mass. We have found mixed results when the repeatabilities of stations coordinates are compared with and without explicit translation and scale parameters, and we leave this question unresolved and awaiting further study.

Acknowledgments. We are grateful to R. Bennett and S. McClusky for providing the GPS quasi-observation data, to M. Lisowski for providing the USGS EDM data and assisting in identification of outliers, and to M. Murray, M. Hefflin and Z. Shen for helpful discussion. The maps in this paper were generated using the public domain Generic Mapping Tools (GMT) software [Wessel and Smith, 1995]. This research was supported at MIT by grants from the National Science Foundation (NSF) (EAR-86-18513 and EAR-89-05560) and the National Aeronautics and Space Administration (NASA) (NAS-5-538 and NAS-5-737); at JPL by contract from NASA; and at both institutions by the Southern California Earthquake Center (SCEC), funded under NSF Cooperative Agreement EAR-8920136 and U. S. Geological Survey Cooperative Agreement 14-8-001-A0899. This paper is paper number 356 of the Southern California Earthquake Center.

REFERENCES

- Bawden, G. W., A. Donnellan, L. H. Kellogg, D. Dong, and J. B. Rundle, Geodetic measurements of horizontal strain near the White Wolf fault, Kern County, California, 1926-1993, in press, *J. Geophys. Res.*, 1996.
- Bennett, R. A., Global Positioning System measurements of crustal deformation across the Pacific-North American plate boundary in southern California and northern Baja, Mexico, Ph. D. thesis, 205 pp., Mass. Instit. of Tech., Cambridge, 1995.
- Bennett, R. A., R. E. Reilinger, W. Rodi, Y. Li, M. N. Toksoz, and K. Hudnut, Coseismic fault slip associated with the 1992 M_w 6.1 Joshua Tree, California earthquake: Implications for the Joshua Tree-Landers earthquake sequence, *J. Geophys. Res.*, 100, 6443-6462, 1995.
- Beutler, G., I. I. Mueller, and R. E. Neilan, The International GPS Service for Geodynamics: development and start of official service on January 1, 1994, *Bull. Geodesique*, 68, 39-70, 1994.
- Bibby, H. M., Unbiased estimate of strain from triangulation data using the method of simultaneous reduction, *Tectonophysics*, 82, 161-174, 1982
- Bierman, G. J., *Factorization methods in discrete sequential estimation, Mathematics in Engineering*, Vol. 128, Academic Press Inc., San Diego, CA., 1977

- Blewitt, G., Y. Bock, and G. Gendt, Regional clusters and distributed processing, *Proceedings of the IGS Analysis Center Workshop*, Ottawa, October 12-14, 1993
- Bock, Y., S. A. Gourevitch, C. C. Counselman III, R. W. King, and R. I. Abbot, Interferometric analysis of GPS phase observations, *Man. Geod.*, 11, 282-288, 1986.
- Bock, Y. D. Agnew, P. Fang, J. Genrich, B. Hager, T. Herring, K. Hudnut, R. King, S. Larsen, J.-B. Minster, K. Stark, S. Wdowinski, and F. Wyatt, Detection of crustal deformation related to the Landers earthquake sequence using continuous geodetic measurements, *Nature*, 361, 337-340, 1993.
- Brunner, F. K., On the analysis of geodetic networks for the determination of the incremental strain tensor, *Surv. Rev.*, XXV(192), 56-67, 1979
- Caspary, W. F., Concepts of network and deformation analysis, *Monograph 11, School of Surveying the University of New South Wales, Kensington, N.S.W., Australia*, 1987
- Collier, P. A., B. Eissfeller, G. W. Hein and H. Landau, On a four-dimensional integrated geodesy, *Bull. Geod.*, 62, 71-91, 1988
- Davis, J. L. et al., Geodesy by radio interferometry: effects of atmospheric modeling errors on estimates of baseline length, *Radio Sci.*, 20, 1593-1607, 1985
- Dong, D., The horizontal velocity field in southern California from a combination of terrestrial and space-geodetic data, Ph. D. Thesis, 157 pp., Massachusetts Institute of Technology, 1993.
- Drew, A. R. and R. A. Snay, DYNAP: software for estimating crustal deformation from geodetic data, *Tectonophysics*, 162, 331-343, 1989
- Feigl, K. L., D. C. Agnew, Y. Bock, D. Dong, A. Donnellan, B. H. Hager, T. A. Herring, D. D. Jackson, T. H. Jordan, R. W. King, S. Larsen, K. M. Larson, M. Murray, Z. Shen, and F. H. Webb, Space geodetic measurement of crustal deformation in central and southern California, 1984-1992, *J. Geophys. Res.*, 98, 21677-21712, 1993
- Grant, D. B., Combination of terrestrial and GPS data for Earth deformation studies, Ph. D. Theses, *Unisurv report S-32*, 1990
- Hager, B. H., R. W. King, and M. H. Murray, Measurement of the crustal deformation using the Global Positioning System, *Annu. Rev. Earth Planet. Sci.*, 19, 351-382, 1991
- Hefflin, M. B., W. I. Bertiger, G. Blewitt, A. P. Freedman, K. J. Hurst, S. M. Lichten, U. J. Linqwister, Y. Vigue, F. H. Webb, T. P. Yunck, and J. F. Zumberge, Global geodesy using GPS without fiducial sites, *Geophys. Res. Lett.*, 19, 131-134, 1992
- Hein, G. W., Integrated geodesy state-of-the-arc 1986 reference text, *Lecture Notes in Earth Sciences*, Vol. 7, 505-548, Edited by H. Sunkel, Springer-Verlag, 1986
- Herring, T. A., Precision and accuracy of intercontinental distance determinations using radio interferometry, *Ph. D. Thesis*, Massachusetts Institute of Technology, 1983

- Herring, T. A., J. L. Davis, and I. I. Shapiro, Geodesy by radio astronomy: the application of kalman filtering to very long baseline interferometry, *J. Geophys. Res.*, 95, 12561-12581, 1990
- Herring, T. A., D. Dong, and R. W. King, Sub-milliscsedon determination of pole position using Global Positioning System data, *Geophys. Res. Lett.*, 18, 18931896, 1991.
- Herring, T. A., GLOBK: Global Kalman filter VLBI and GPS analysis program, unpublished documentation, MIT, 1995
- Hudnut, K. W., Y. Bock, M. Cline, P. Fang, Y. Feng, J. Freymueller, X. Ge, W. K. Gross, D. Jackson, M. Kim, N. E. King, J. Langbein, S. C. Iarsen, M. Lisowski, Z. Shen, J. Svarc, and J. Zhang, Co-seismic displacements of the 1992 Landers earthquake sequence, *Bull. Seis. Soc. Amer.*, 84, 625-645, 1994.
- Hudnut, K. W., Z. Shen, M. Murray, S. McClusky, R. King, T. Herring, B. Hager, Y. Feng, P. Fang, A. Donnellan, and Y. Bock, Co-seismic displacements of the 1994 Northridge, California, earthquake, *Bull. Seis. Soc. Amer.*, 86, 519-536, 1996.
- International Earth Rotation Service, *IERS Standards (1992)*, IERS Technical Note 13, D. D., McCarthy, edit., Observatoire de Paris, July, 1992.
- Jackson, D. D., The use of a priori data to resolve non-uniqueness in linear inversion, *Geophys. J. R. astr. Soc.*, 57, 137-157, 1979
- Jackson, D. D., and M. Matsu'ura, A Bayesian approach to nonlinear inversion, *J. Geophys. Res.*, 90, 581-591, 1985
- Johnson, H. O., D. C. Agnew, and F. K. Wyatt, Present-day crustal deformation in southern California, *J. Geophys. Res.*, 99, 23951-23974, 1994
- King, N. E., J. L. Svarc, E. B. Fogleman, W. K. Gross, K. W. Clark, G. D. Hamilto, C. H. Stiffler, and J. M. Sutton, Continuous GPS observations across the Hayward fault, California, 1991-1994, *J. Geophys. Res.*, 100, 20271-20284, 1995
- King, R. W., and Y. Bock, Documentation for the MIT GPS analysis software: GAMIT, Massachusetts Institute of Technology, 1992
- King, R. W., E. G. Masters, C. Rizos, A. Stolz, and J. Collins, Surveying with GPS, *Monogr. Ser.*, vol. 9, School of Surveying, University of New South Wales, New South Wales, Australia, 1985
- Lisowski, M., J. C. Savage and W. H. Prescott, The velocity field along the San Andreas fault in central and Southern California, *J. Geophys. Res.*, 96, 8369-8389, 1991
- MacMillan, D. S., and C. Ma, Atmospheric gradients and the VLBI terrestrial reference frame, *Geophys. Res. Lett.*, submitted, 1996.
- Milbert, D. G. and W. T. Dewhurst, The Yellowstone-Hebgen lake geoid obtained through the integrated geodesy approach, *J. Geophys. Res.*, 97, 545-558, 1992

- Oral, M. B., R. E. Reilinger, M. N. Toksoz, R. W. King, A. A. Barka, I. Kinik, and O. Lenk, Global Positioning System offers evidence of plate motions in eastern Mediterranean, *Eos Trans. AGU*, 76, 9, 11, 1995.
- Prescott, W. H., An extension of Frank's method for obtaining crustal shear strains from survey data, *Bull. Seismol. Soc. Am.*, 66, 1847-1853, 1976
- Prescott, W. H., The determination of displacement field from geodetic data along a strike slip fault, *J. Geophys. Res.*, 86, 6067-6072, 1981
- Reilinger, R., J. Beavan, L. Gilbert, S. Larsen, K. Hudnut, C. Aiken, D. Ziegler, W. Strange, M. Fuente, J. Carcia, J. Stowell, W. Young, G. Doyle, and G. Stayner, 1990 Salton Trough-Riverside County GPS Network (abstract), *Eos. Trans. AGU*, 71, *Spring Meeting Suppl.*, 477, 1990.
- Savage, J. C. and W. H. Prescott, Precision of geodolite distance measurements for determining fault movements, *J. Geophys. Res.*, 78, 6001-6008 1973
- Savage, J. C., W. H. Prescott, and G. Gu, Strain accumulation in southern California, 1973-1984, *J. Geophys. Res.*, 91, 7455-7473, 1986
- Savage, J. C., and M. Lisowski, Geodetic monitoring of the southern San Andreas fault, California, 1980-1991, *J. Geophys. Res.*, 100, 8185-8192, 1995
- Savage, J. C., M. Lisowski, and W. H. Prescott, Observed discrepancy between Geodolite and GPS distance measurements, *J. Geophys. Res.*, 101, 25547-25552, 1996
- Segall, P. and M. V. Matthews, Displacement calculation from geodetic data and the testing of geophysical deformation models, *J. Geophys. Res.*, 93, 14954-14966, 1988
- Shen, Z. K., Regional tectonic deformation in southern California, inferred from terrestrial geodesy and the Global Positioning System, Ph.D. thesis, UCLA, 1991
- Shen, Z. K., D. D. Jackson, Y. Feng, M. Cline, M. Kim, P. Fang, and Y. Bock, Postseismic deformation following the Landers earthquake, California, 28 June 1992, *Bull. Seism. Soc. of Amer.*, 84, 780-791, 1994
- Snay, R. A. and A. R. Drew, Combining GPS and classical geodetic surveys for crustal deformation in the Imperial Valley, California, *High Precision Navigation -- Integration of Navigational and Geodetic Methods*, Springer-Verlag, New York, 225-236, 1989
- Snay, R. A., M. W. Cline and E. L. Timmerman, Project REDEAM: Models for Historical Horizontal Deformation, *NOAA Technical Report NOS 125 NGS 42*, 1987
- SOPAC staff, Scripps Orbital Processing and Analysis Center and Southern California Permanent GPS Array, in *Proc. of National Research Council*, in press, 1996
- Vanicek, P., and E. Krakiwsky, Geodesy: the concepts, second edition, *North-holland*, 1986
- Wessel, P., and W. H. F. Smith, New version of the Generic Mapping Tools released, *EOS Trans. Am. Geophys. U.*, 76, 329, 1995.

- Zhang, J., Y. Bock, and P. Fang, Distributed analysis of global positioning system networks, submitted to *Geophys. Res. Lett.*, 1996a.
- Zhang, J., Y. Bock, H. Johnson, P. Fang, S. Wdowinski, J. F. Ginrich, and J. Behr, Southern California Permanent GPS Geodetic Array: error analysis of daily position estimates and site velocities, submitted to *J. Geophys. Res.*, 1996b
- Zhao, S-R, and L. E. Sjoberg, Theory for inversion of integral equations with constraints: mathematical rationale and some applications to geodetic data, *Manuscripta geodaetica*, 10, 278-299, 1995
- Zumberge, J., M. B. Hefflin, D. C. Jefferson, M. M. Watkins, and F. H. Webb, Precise point positioning for the efficient and robust analysis of GPS data from large networks, *J. Geophys. Res.*, in press, 1996

Table 1. Primary observations used in the combined analysis

Survey	Condition number ^a	$\delta\chi^2$	
		forward	backward
<u>GPS</u>			
Salton Trough / Riverside County	<i>Bennett [1995]</i>		
STRC88	9.5×10^7	0.006	1.565
STRC90	5.9×10^7	0.126	1.570
STRC91	NPD ^b	1.574	1.185
JTRE92 (pre-EQ)	1.3×10^8	1.311	1.211
JTRE92 (post-EQ)	2.6×10^8	0.915	0.855
STRC93	5.4×10^{10}	0.452	0.701
STRC95	6.4×10^{10}	3.297	1.433
Intercounty IC93	<i>Hudnut et al. [1996]</i>		
IC93 Ashtech subset	5.6×10^7	0.416	1.217
IC93 Trimble subset	NPD ^b	0.735	0.211
IC93 global subset	5.1×10^8	3.054	3.991
IC93 PGGA subset	5.6×10^8	3.570	0.120
Mexicali Valley	<i>Bennett [1995]</i>		
GEOMEX 89	1.1×10^8	2.316	6.636
Transverse Ranges	<i>Feigl et al., [1993]</i>		
TREX00 (June, 1986)	1.2×10^8	0.022	2.029
TREX10 (March, 1988)	1.9×10^8	0.170	1.565
TREX13 (March, 1989)	2.4×10^8	1.293	4.233
TREX14 (March, 1989)	2.2×10^8	0.845	1.420
TREX16 (March, 1989)	1.2×10^5	2.454	2.468
TREX18 (March, 1990)	5.9×10^7	3.246	1.126
TREX20 (March, 1991)	9.3×10^7	4.250	0.271
Santa Barbara Channel	<i>Feigl et al. [1993]</i>		
SBC91	3.2×10^7	1.574	1.185
<u>EDM</u>			
Joshua Tree (1974-1992)	<i>Lisowski et al. [1991]</i>		
Anza (1973-1991)			
Salton (1972-1991)			
Monitor (1974-1990)			

^a Condition number is estimated as the ratio of the maximum eigenvalue over the minimum eigenvalue of the covariance matrix of the loosely constrained quasi-observations.

^b The covariance matrices for these quasi-observations were non-positive definite (NPD), for reasons that are unclear. We removed the singularity by adding diagonal consider covariance matrices with diagonal terms $(4 \text{ mm})^2$ and $(3 \text{ mm})^2$ for STRC91 and the IC93 Trimble subset, respectively. Adding small terms to the diagonals keeps the large eigenvalues of the original covariance matrices unaffected while effectively masking the smallest eigenvalues.

Table 2. Earthquake parameters used in the analysis of the southern California data

Event ^a	Date	Magnitude	Depth (km)	Constraint (m)			Range (km)
				east	north	up	
Homestead Valley	Mar 15, 1979	5.6	10.0	0.2	0.2	0.5	30
Westmoreland	Apr 26, 1981	5.7	10.0	0.2	0.2	0.5	30
N. Palm Springs	Jul 8, 1986	6.0	10.0	0.5	0.5	1.0	50
Superstition Hills	Nov 24, 1987	6.2	10.0	0.5	0.5	1.0	80
Joshua Tree	Apr 22, 1992	6.1	10.0	0.05	0.05	0.2	80.0
Landers	Jun 28, 1992	7.5	15.0	2.0	2.0	5.0	500.0
Northridge ^b	Jan 17, 1994	6.7	10.0	0.25	0.25	0.5	200.0

^a We do not assign a priori values for the first 4 earthquake induced displacements. Thus we set larger constraint values for the coseismic displacements.

^b Since the Northridge earthquake influenced only a few stations close to the northwestern boundary of our region at the level less than 0.4 mm based on the model of *Hudnut et al.* [1996], we used the model-predicted values as the a priori values of the coseismic displacements at these stations and assign the constraints as 100% of the model predicted values.

Figure captions

Figure 1. Effects of applying a priori constraints on height estimates in a loosely constrained GPS analysis. Results from two stations are shown, one in North America (large closed circles) and one in Tibet (large open circles). These results were generated by applying a 1 m height change to the a priori coordinates of each station, and analyzing the GPS quasi-observations with standard deviations assigned to these heights ranging from 1000 to 1 mm. All other sites in the analysis were constrained with standard deviations of ± 100 m. The thick dotted lines show the effects of these constraints from *Herring et al.* [1990]. (The stippled curve for the closed circle results is overlain by the open circle results.) The thin lines and small circles show the ratio of the height error from the analysis and the predicted error. The prediction is always within a factor of 2 for this analysis.

Figure 2. Map of southern California showing the GPS station (triangles) and USGS EDM networks (named with italics and linked with solid lines). The main tectonic domains and faults are labeled with bold italics: eastern California shear zone (ECSZ), Ventura Basin (VB), southern Borderlands (SBL), San Andreas fault (SAF), San Jacinto fault (SJC), Elsinore fault (ELS), Cerro Prieto fault (CPR), and San Clemente fault (SCL).

Figure 3. GPS-derived velocity field relative to a reference frame fixed to the North American plate. The error ellipses are constructed from the one sigma uncertainties of the horizontal components and hence represent regions of 39% confidence in two dimensions. The a priori errors assigned to the GPS data (see text) have been rescaled by a factor of 1.82 to make the chi-square per degree of freedom equal to unity.

Figure 4. GPS/EDM combined velocity field relative to North America plate fixed frame. The GPS errors have been scaled by a factor of 1.82, and the EDM by 1.22 prior to combination (see text). Error ellipses are the same as in Figure 3.

Figure 5. Enlargement of the GPS-only (a) and combined (b) velocity fields shown in Figures 3 and 4.

Figure E.1. Changes in the lengths of the baselines when the constraints in equation (E.4a) are applied to a GPS analysis in which there are no explicit translation or scale parameters. The cases shown are (a) 1 m X translation, (b) 1 m Y translation, (c) 1 m Z translation and (d) 160 ppb scale change (equivalent to 1 m height changes).

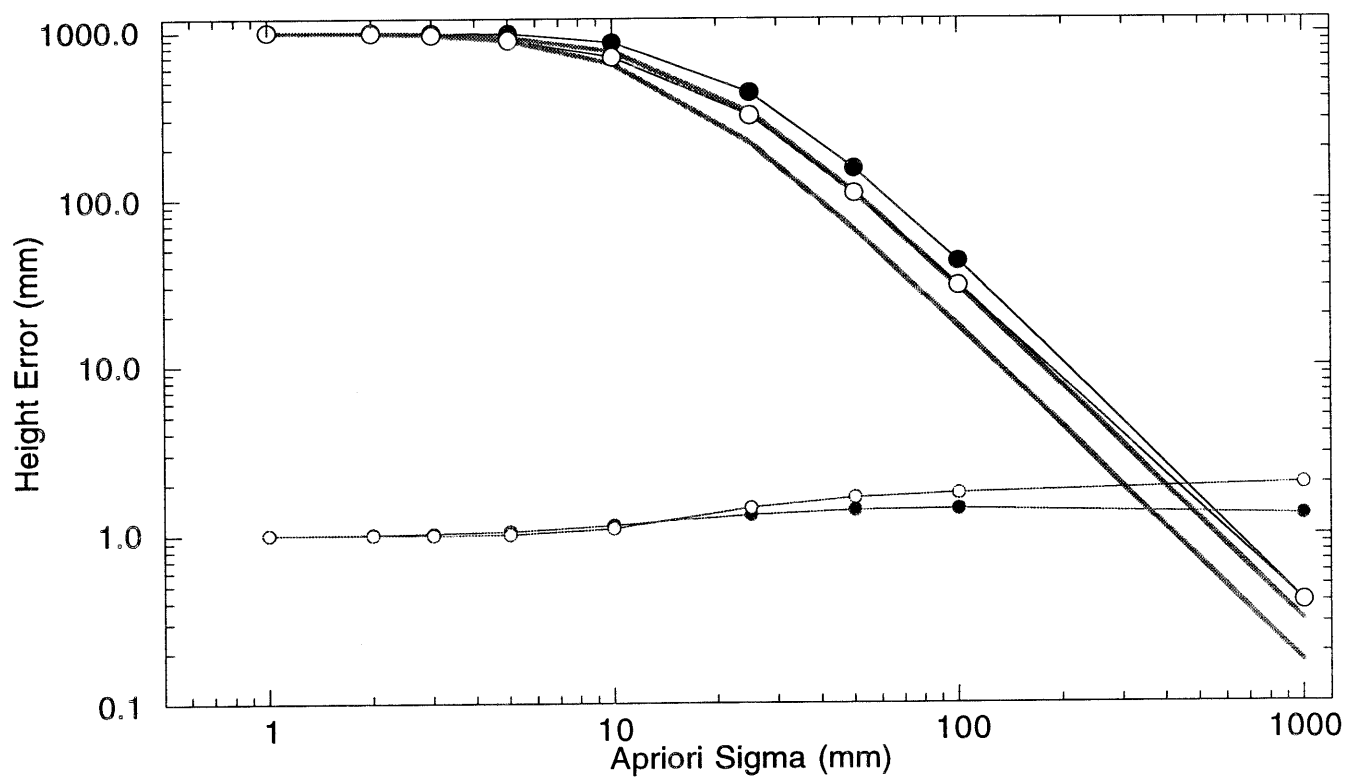


Figure 2

(with multiple epoch observations)

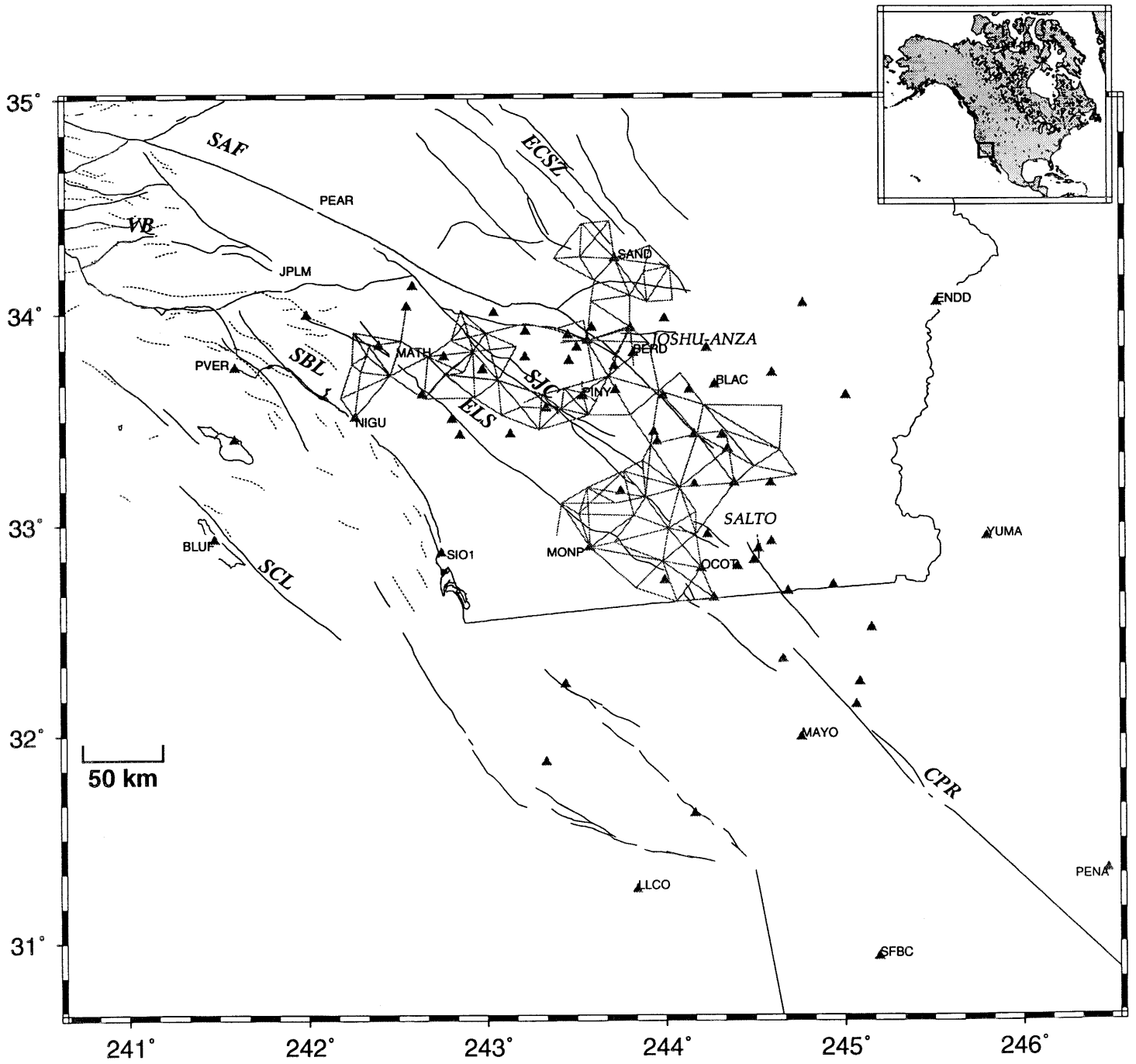


Figure 3

39% confidence

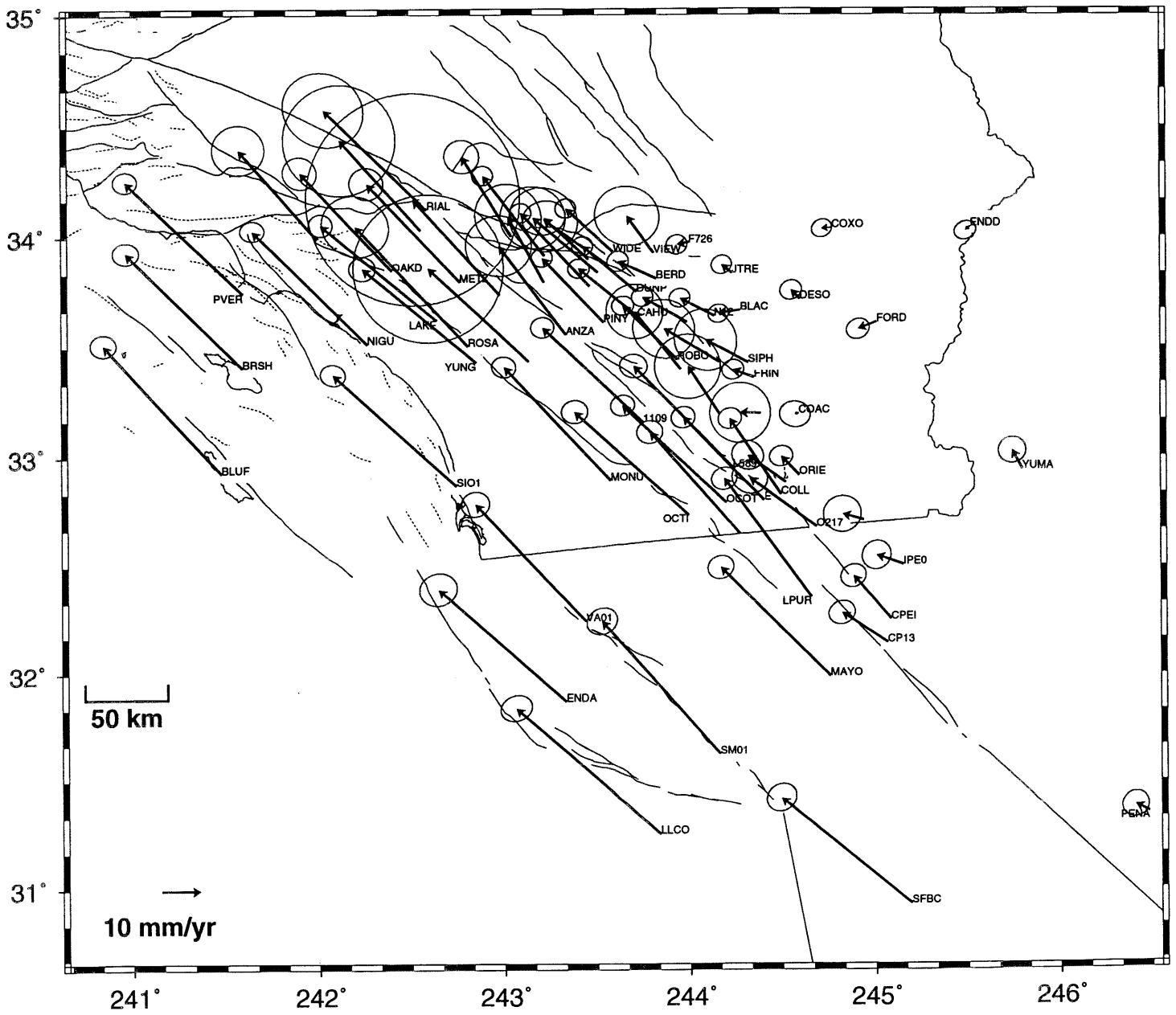


Figure 5a

39% confidence

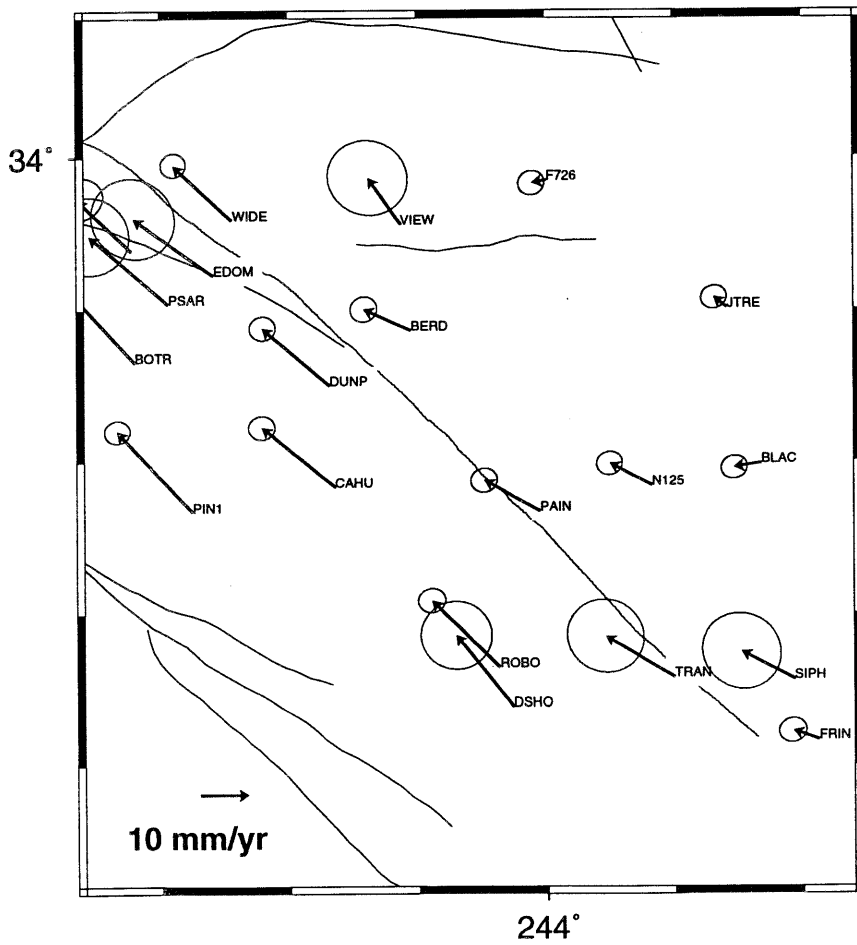


Figure 5b

39% confidence

